SOVIET PHYSICS USPEKHI VOLUME 12, NUMBER 2 SEPTEMBER-OCTOBER 1969

538.7

GEOMAGNETIC PULSATIONS AND DIAGNOSTICS OF THE MAGNETOSPHERE

V. A. TROITSKAYA and A. V. GUL'EL'MI

Borok Geophysical Observatory; Institute of Earth Physics, USSR Academy of Sciences

Usp. Fiz. Nauk 97, 453-494 (March, 1969)

1. INTRODUCTION

ELECTROMAGNETIC waves of very low frequency are incident on the earth's surface from outer space. These waves, called "geomagnetic pulsations," were first observed at the Kew Observatory near London approximately a hundred years ago. However, a thorough study of the pulsations began only during the International Geophysical Year (1957-1958)[1].

Geomagnetic pulsations are hydromagnetic waves in the earth's magnetosphere. The frequency spectrum extends from several millihertz to approximately 1 kilohertz. The lower limit of the spectrum coincides with the lowest frequency of the natural oscillations of the magnetosphere, and the upper limit with the gyrofrequency of the protons in the lower layers of the polar ionosphere. At a frequency of approximately 5 Hz, however, there is a sharp cutoff of the oscillation spectrum, due to the fact that the upward-traveling waves are strongly absorbed in the ionosphere and are practically not observed on the earth's surface. In addition, at frequencies larger than approximately 5 Hz, the level of the atmospheric noise due to thunderstorm discharges is quite high, and this also hinders the registration of radiation of cosmic origin. It has therefore been concluded on the basis of the observed material that the upper limit of the magnetic pulsations lies at several Hz.

Starting with frequencies of several hundred Hz, the ionosphere again becomes transparent and the level of the cosmic noise increases. This is the lower limit of the very low frequency (VLF) band.*

The maximum intensity of VLF radiation occurs at a frequency of several kHz. In spite of this difference between their frequencies, the micropulsations and the VLF radiation have features that are physically and formally common[2], and form jointly the low-frequency band of natural electromagnetic radiation (Fig. 1).

Two reviews dealing with VLF radiation have already been published in this journal[3,4]. On the other hand, the investigations of pulsations have not yet been described in the domestic review and monographic literature. At the same time, an increasing flow of information concerning geomagnetic pulsations has been observed in recent years (see, for example, the reviews[1,5-12]).

The purpose of the present review is to report to the readers the results and prospects of investigations of the pulsations, which constitute an interesting and still puzzling natural phenomenon.

Observation of the pulsations is one of the main in-

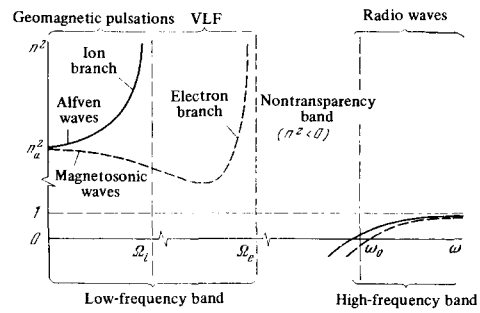

FIG. 1. Dispersion curves for transverse waves in a magnetoactive plasma: n – refractive index, ω_0 – plasma frequency, Ω_e and Ω_i – electron and ion gyrofrequencies.

direct proofs of the existence of hydromagnetic waves in the earth's magnetosphere. The pulsations serve as convenient tests of various theories of excitation and propagation of waves in a plasma. Moreover, the interpretation of pulsations raises new problems, thereby serving as a definite stimulus to the development of the theory of plasma waves. The main results of the observations of geomagnetic pulsations and the existing theories of their origin are reported in the first part of the review.

Recently, interest has been evinced in pulsations as a source of information concerning the parameters of the magnetosphere and of the solar corpuscular streams. Being excited at high altitudes, the hydromagnetic waves bring to the earth's surface valuable information concerning the conditions in outer space. Thus, observation of the pulsations may become one of the means of diagnosing the state of the interplanetary medium and the parameters of the magnetosphere in the regions where the waves are generated and on their path of their propagation towards the earth's surface. This new trend in the investigation of the pulsations (to which the second part of the review is devoted) has developed for the greater part as a result of the work done at the Division of the Earth's Electromagnetic Field and the Borok Geophysical Observatory of the Earth-physics Institute of the USSR Academy of Sciences[8-10,13-17]. Although the work on diagnostics is still mainly methodological, a review of this work gives an idea of the prospects of further research.

II. GEOMAGNETIC PULSATIONS

There is a large variety of the types of pulsations, differing from one another in spectral composition, time evolution, character of distribution over the earth's surface, etc. They are registered by means of sensitive magnetometers of various designs[12]. The instruments were installed in an extensive network of observatories covering the entire earth more or less

*In analogy with the VLF radiation, pulsations in the frequency range from several millihertz to several hertz are sometimes called ultra-low frequency (ULF) radiation.

uniformly and recording their data continuously. The initial data obtained in this manner are used to study the spectrum, polarization, and coherence of the oscillations, and also for traditional geophysical investigations, namely the analysis of the diurnal, 27-day, seasonal, and 11-year variations, the dependence of the properties of the pulsations on the solar and geomagnetic activity, etc.

Modern methods of investigating the pulsations are characterized by the organization of special experiments aimed at verifying and refining various theoretical models. A decisive role in the clarification of the nature of several types of pulsations was played by observations in conjugate* and antipode points, at the geomagnetic poles, and on the equator[18-20]. A comprehensive program aimed at comparing the pulsation spectra with satellite measurements of the parameters of outer space is also being successfully realized[8-10].

There is no complete theory of geomagnetic pulsations at present. The general principles of the physical interpretation have been established, and individual properties of the pulsations have been explained. The complexity and variability of the structure of the near-earth space make it difficult to formulate and solve concrete problems rigorously. Therefore, approximate and tentative calculations are extensively used, as well as a general qualitative analysis of the processes of excitation and propagation of the pulsations.

It has become more and more obvious of late that further development of the theory of geomagnetic pulsations is possible only in direct association with rigorously formulated experiments. Of great importance, in particular, will be simultaneous observations of pulsations on the earth's surface and directly in outer space. The observations made until recently were sporadic and incomplete.

1. Main Properties of Pulsations

Let us consider briefly the classification of geomagnetic pulsations. A classification is necessary in order to represent the variety of types of oscillations by a limited number of ordered and well identified types.

In the literature there have been discussed essentially three independent principles of classification (Fig. 2):

1) A classification based on morphological attributes (periods, amplitudes, times of appearance, etc.).

2) Correlative classification (in connection with other phenomena—magnetic storms, auroras, VLF radiation, etc.).

3) Genetic classification, based on the production mechanisms. Inasmuch as the actual nature of the pulsations is still far from clear, the genetic classification, which under other circumstances would be preferable, cannot serve as the basis of a general classification. The correlative principle can likewise not serve as a basis, since not all types of oscillations reveal a pronounced correlation. Consequently, the morphological classification principle, first clearly formulated in[21], has gained extensive and justified

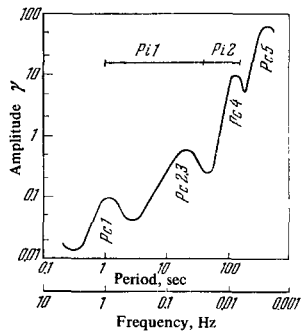

FIG. 2. Spectrum of geomagnetic pulsations (schematic representation [12]).

Table I

Type	Range of periods, sec
Stable pulsations	
Pc1	0.2—5
Pc2	5—10
Pc3	10—45
Pc4	45—150
Pc5	150—600
Irregular pulsations	
Pi1	1—40
Pi2	40—150

recognition. The morphological classification adopted at the 13th General Assembly of International Year of the Quiet Sun (August 1963, Berkley, California[22,23]) is presently in use.

The oscillations are subdivided into two main classes: regular (stable) and irregular. The regular oscillations are quasisinusoidal, stable, and are denoted Pc (pulsations, continuous). The class Pc is divided in turn into five spectral subclasses. The class of irregular oscillations, Pi (pulsations, irregular), contains two subclasses (Table I). In the discussion of the concrete types of pulsations, additional designations are frequently used (pearls, hydromagnetic hiss, etc.)

1.1. Pearls. The term "pearls" was proposed to denote series of quasi-monochromatic pulsations in the Pc1 range[1]. An oscillogram of the oscillations actually recalls a string of pearls (Fig. 3a). The signal repetition period is $\tau \sim 1-4$ min. The average oscillation frequency is connected with the repetition period by a relation of the type $\tau f \approx 10^2$. The oscillation amplitude is of the order of ~10—100 $m\gamma$[8-12,24-38].

The envelopes of the signals in magnetically-conjugate points are approximately 180° out of phase. In other words, the pearl appears alternately on opposite ends of the geomagnetic-field line[9,18,25,26]. Figure 3a illustrates this important feature of the pearl. The signals were recorded at the conjugate points Sogra (a settlement in the Arkhangel'sk region) and Kerguelen (an island in the Indian Ocean)[18].

Sometimes the investigated pearls are distinctly separated in time. More frequently, however, the signals overlap each other, producing a complicated picture of beads. Such pearls are best analyzed with the aid of a sonograph—an instrument for the construction of the dynamic spectrum of oscillations[24]. Figure 3b shows a typical sonogram of a series of pearls. The

*A pair of points on the earth's surface is called conjugate if they are joined by a force line of the geomagnetic field.

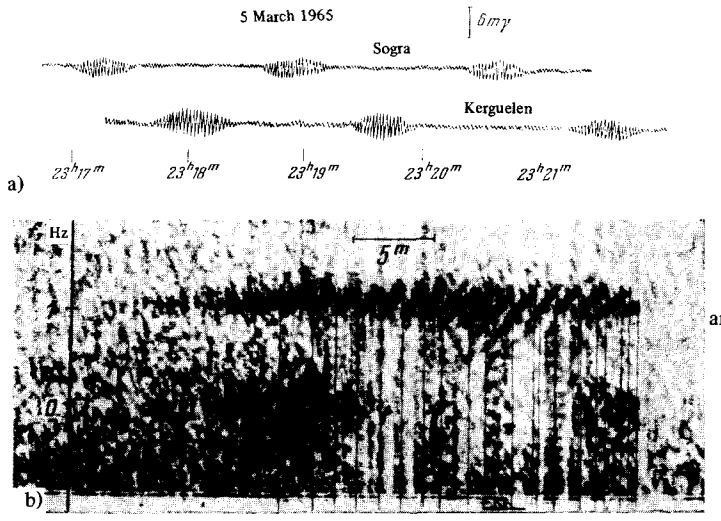

FIG. 3. Oscillogram of pearl in magnetically conjugate points Sogra and Kerguelen (a) and dynamic spectrum of the pearl (b).

vertical axis represents the frequency and the horizontal time, while the spectral density of the oscillations is proportional to the density of the plot. Sonograms of the same series become identical at conjugate points if they are shifted in time relative to each other by half the repetition period.

An analysis of the dynamic spectra shows that in the overwhelming majority of cases the series of pearls consist of discrete tones of increasing frequency. The occasionally observed series of signals with decreasing frequency are more readily the exception than the rule. The typical slope of the structure elements is $df/dt \sim 0.1$ Hz/min[25]. A slow change of the slope, i.e., a dispersion effect, becomes noticeable in the course of time at the end of the series. The relative bandwidth of isolated series is comparatively small: $\Delta f/f \sim 0.2$. Broad bands are observed upon appearance of several series that proceed simultaneously in different sections of the spectrum.

The polarization of the bead in the horizontal plane is elliptic, and the parameters of the ellipse vary slowly in time, as expected when account is taken of the fact that the pearls are not fully monochromatic. It is reported in[27] that in conjugate points the horizontal projection of the magnetic-field perturbation vector h rotates in opposite directions. The north-south component of the vector h is usually larger in absolute magnitude than the east-west component. There are indications that the ratio h_{N-S}/H_{W-E} increases with decreasing geomagnetic latitude of the point of observation[28,29].

Pearls with periods $T > 2-3$ sec appear locally, and those with periods $T < 2$ sec appear as a rule globally, i.e., they appear in observatories that are far from each other[8,30]. Cases are known when pearls were simultaneously observed at medium latitudes and on the equator[25], and also at both geomagnetic poles[19]. Precision measurements have established that the pearls propagate along the earth's surface from the subauroral latitudes in the direction towards the equator with a velocity ~700–900 km/sec[31,32].

Pearls are a rather rare phenomenon. They occur sporadically and last on the average about a half-hour. Sometimes, incidentally, series of pearls continue for many hours. A complicated diurnal-latitudinal variation in the probability of the appearance of pearls is observed[9,12,33]. The maximum appearance probability occurs in early morning hours and at noontime at medium and high latitudes respectively. A slight increase of the probability of appearance begins approximately one hour after the sudden commencement of a magnetic storm (ssc)[1]. Frequently the pearls occur also 1–3 minutes after ssc and last approximately ~40 minutes[34,35]. In such cases, however, the dynamic spectrum of the oscillations is quite smeared out and irregular. If, owing to random factors, the ssc occurs during the time of a series of pearls, then the signal carrier frequency increases jumpwise by $\Delta f \sim 0.1-0.3$ Hz[34].

Sudden starts of the storms (and also sudden pulses of the magnetic field, si) are associated with only a small fraction of the total number of series of pearls. There are reports in the literature that pearls have a certain tendency to appear in days when the earth is on the boundary between the sectors of the interplanetary magnetic field[36]. However, for example, no direct connection was observed between the appearance of pearls and the Kp-index of the geomagnetic activity. It is only known that a large number of pearls appear during the first week after a magnetic storm[37,38]. Many years of observations have also established that the probability of occurrence of the pearl has a maximum during the decreasing section of the 11-year cycle of solar activity[30].

A distinguishing feature of pearls is the absence of a distinct connection between the instant of their occurrence and other manifestations of geomagnetic activity. This puzzling arbitrariness in the excitation of the pearls has been the stimulus for an extensive literature. So far, however, it was impossible to observe the agent stimulating the excitation of the pearl (with the exception of ssc). An impression is gained that the instant of generation is preceded by a certain preparatory stage of processes that are difficult to capture.

1.2. Random pulsations

Auroras are characterized by geomagnetic noiselike

variations in the Pi1 band. These irregular pulsations come in a great variety of types and are usually accompanied by pulsations, having a similar spectrum, in the flux of x-rays in the stratosphere, in the aurora glow intensity, etc. The Pi1 activity increases following the appearance of magnetic bays, during the time of which there occur also increases in the aurora glow, in the absorption of cosmic radio noise, and in ionospheric disturbances[1,12]. The main cause of this entire set of phenomena are fluctuating fluxes of electrons with energies ~10 keV, which bombard the polar ionosphere[39]. Figure 4 shows an example of the close connection between Pi1 and the fluctuations of the aurora glow[12].

At times, short pulsed bursts of oscillations appear near local midnight (Fig. 5). The duration of the individual pulses is ~1–2 min. Unlike pearls, Pi1 bursts have a broad spectrum and are observed simultaneously in conjugate points[18,40]. They reveal a tendency to occur in groups of 3–5 pulses with an interval ~5–15 min. The most interesting feature is the quasiperiodicity of the bursts. The repetition period of the bursts shown in Fig. 5 is $\tau \approx 10$ min.

During the principal phase of geomagnetic storms, at evening and pre-midnight hours, broadband pulsations with slowly increasing average frequency are observed[9,41-43] (Fig. 6). During approximately one half hour, the frequency grows from a fraction of a hertz to several hertz: $df/dt \sim 5 \times 10^{-4}$ Hz/sec. The growth of the frequency is accompanied by a sharp increase of the magnetic activity, by a shift of the lower limit of the aurora zone to the equator, by the spilling of particles from the radiation belts, etc. Figure 7 shows an example of a comparison of pulsations of increasing frequency with data obtained from satellite measurements of the radiation-belt parameters[9].

Let us indicate one more type of pulsation—"hydromagnetic hiss"—which can be arbitrarily assigned to the Pi1 band. On the sonogram they have the appearance of a broad band centered at the frequency ~0.5 Hz[44]. Hydromagnetic hiss occurs during the night against a relatively quiet magnetic background, and has no fine structure.

1.3. Long-period pulsations Pc2–5 and Pi2. Pc2 4 pulsations are observed continuously on the earth's surface facing the sun. This is the most widespread form of pulsation (Fig. 8a). The amplitude of the oscillations (on the order of ~1–10 γ) decreases with increasing distance from the noon meridian and, at least within the limits of the medium-latitude belt, it increases with increasing geomagnetic latitude. The period of simultaneously occurring oscillations is practically the same on the entire daytime hemisphere[5-9,45,46].

Pi2 pulsations are observed in the form of trains on the night side of the earth (Fig. 8b). The Pi2 amplitude (on the order of ~10 γ) is maximal near the aurora zone during the near-midnight hours. During the night, several trains are observed on each observatory. The number of trains and their amplitude increase during the time of polar magnetic disturbances. Pi2 are quite frequently forerunners of magnetic bays[5-9,47-51].

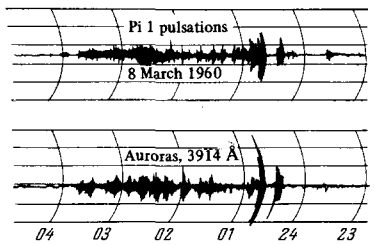

FIG. 4. Simultaneous recording of magnetic pulsations and of the variations of the brightness of polar auroras [12].

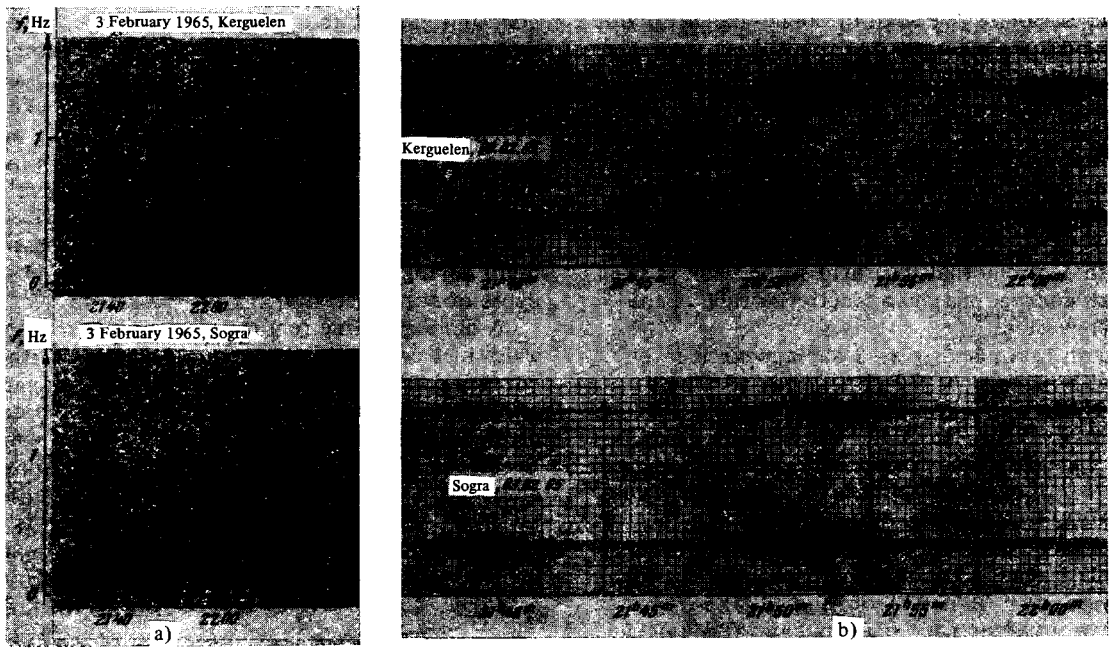

FIG. 5. Pulsed bursts of Pi 1 oscillations in the conjugate points Sogra and Kerguelen.

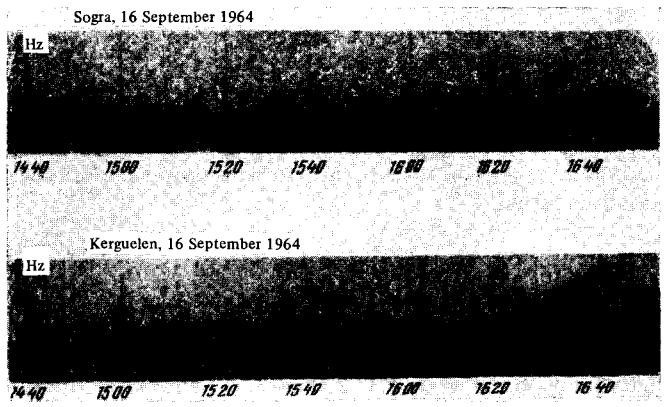

FIG. 6. Pulsations with increasing frequency.

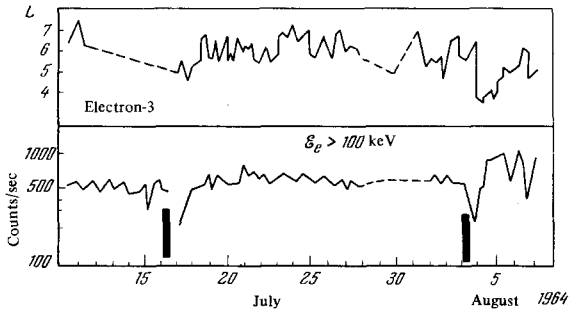

FIG. 7. Occurrence of oscillations of increasing frequency (black vertical strips) during the time of intense variations of the parameter of the outer radiation belt. The lower figure shows the changes of the flux of electrons with energies $\mathcal{E}_e \geq 100$ keV near the maximum of the belt; in the upper figure is shown the boundary of the belt as obtained from the data of the satellite "Electron-3" [9].

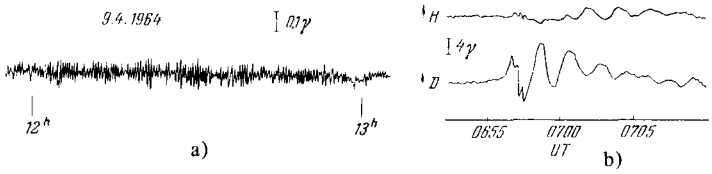

FIG. 8. Long-period pulsations observed during the day (a) and at night (b).

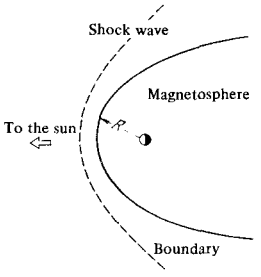

FIG. 9. Equatorial section through the magnetosphere.

The period of the Pc2–4 and Pi2 pulsations decreases monotonically with increasing geomagnetic activity as characterized by the Kp-index. The nature of this effect became clear after interesting comparisons were made between the spectra of the pulsations and satellite data on the position of the boundary of the magnetosphere[13,15,52].

As is well known, the earth's magnetosphere is produced under the influence of streams of solar plasma,

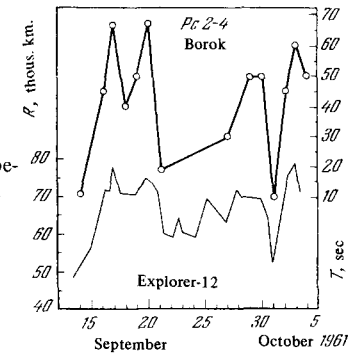

FIG. 10. Comparison of the periods of Pc 2–4 with the position of the boundary of the magnetosphere.

and represents an extensive cavity of complex configuration[53] (Fig. 9). On the subsolar side, the regular magnetic field is bounded by a quasispherical surface at an average distance of 10 earth's radii; a long magnetic tail extends on the opposite side. Direct measurements of the field and of the particle fluxes show that the boundary of the magnetosphere is in constant motion, approaching the earth's surface when the solar wind becomes stronger, and moving away when the wind weakens and the normal pressure on the surface of the cavity decreases. The corresponding position on the boundary on the earth-sun line changes on the average from R ~ 8 to R ~ 12 earth's radii. It turns out that the variation of R is accompanied by a change of the period of the pulsations. A typical example of such a correspondence is shown in Fig. 10. The lower curve shows the position of the boundary of the magnetosphere, measured with the satellite Explorer-12; the upper curve is the period of oscillations of Pc2–4, registered at the medium-latitude observatory Borok[15,46].

Further analysis of surface and satellite data has established the following important regularity: the amplitude of Pc2-4 depends on the orientation of interplanetary magnetic fields[54]. The intensity vector of the interplanetary field is quite stable in magnitude ($H \sim 5-10\gamma$), but varies considerably in direction[53,55]. Figure 11 shows an example of the modulation of the amplitude of Pc3 when the orientation of the interplanetary magnetic field changes in the ecliptic plane. It is seen that the pulsations vanish and their amplitude decreases below the noise level when the azimuthal component of the interplanetary field increases.

The interplanetary field component $H_\perp$ perpendicular to the ecliptic is as a rule several times smaller than the modulus of the ecliptic projection[55]. Nonetheless, the nighttime trains of Pi2 are sensitive to changes of just this component. Trains appear most frequently about 20–40 minutes following the reversal of the direction of H_φ from north to south, and the amplitude of Pi2 is connected in some manner with the magnitude of the $\Delta H_\perp$ jump (Fig. 12)[51].

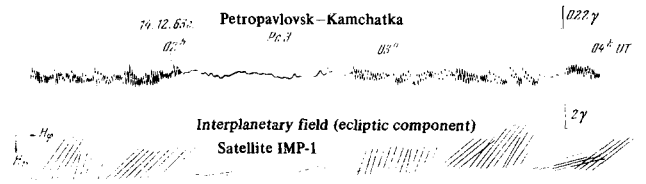

FIG. 11. Modulation of the Pc 2–4 amplitude by the interplanetary magnetic field. H_r and H_φ are the radial and azimuthal components of the interplanetary field in the heliocentric coordinate system.

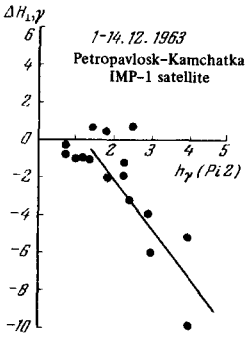

Fig. 12. Connection between amplitude of Pi2 trains and the jump of the interplanetary field.

Oscillations of the type Pc5 are localized in relatively narrow bands stretching along the geometric parallels, and unlike Pc2–4 and Pi2 their period has a sharply pronounced dependence on the latitude φ_0 of the point of observation[56]. In the interval from $\varphi_0 \approx 70°$ to $\varphi_0 \approx 60°$, the period decreases monotonically from $T \sim 500$ sec to $T \sim 200$ sec. There are grounds for assuming that oscillations with an analogous property exist at lower latitudes. At $\varphi_0 < 60°$, under ordinary conditions, they are apparently masked by global pulsations with a period that does not depend on φ_0. At any rate, there are trains of oscillations with a period $T = T(\varphi_0)$, which can be observed up to $\varphi_0 \approx 53°$ are excited in the case of ssc[56-58].

Unfortunately, we are unable to present a complete review of all the pulsation properties revealed as a result of many years of observation. The morphology of the pulsations is described in greater detail in the reviews[8-10] and in the periodic literature.

2. Oscillations and Waves in the Earth's Magnetosphere

The interpretation of geomagnetic pulsations consists primarily of identification of the concrete type of pulsations with definite forms of wave fields in the magnetosphere. Noticeable progress was made recently, although the problem cannot be regarded as completely solved.

The amplitude of the pulsations is small enough to be able to use in first approximation the linear theory of wave propagation in the plasma. In the Pc1 band it is permissible, further, to use the geometrical-optics approximation. However, in the Pc2–5 range the lengths of the hydromagnetic waves are commensurate with the dimensions of the magnetosphere, so that it is necessary to employ other approximate methods or else a numerical calculation. The collisions between particles play an important role at ionospheric altitudes (60–600 km above the earth's surface). In other regions of the magnetosphere, the plasma can be regarded as collisionless.

These preliminary remarks justify the sequence that we shall use in the exposition of the material.

2.1. Wave propagation in the geometrical-optics approximation. The local refractive index of the medium $n = ck/\omega$ is determined by solving the dispersion equation[59-64]

$$\mathrm{Det}\left\{\varepsilon_{\alpha\beta} - n^2\left(\delta_{\alpha\beta} - \frac{k_\alpha k_\beta}{k^2}\right)\right\} = 0, \tag{1}$$

where ω is the frequency of the plane wave $\sim \exp(i\mathbf{k}\cdot\mathbf{r} - i\omega t)$, k_α are the components of the wave vector $\mathbf{k}$, $\delta_{\alpha\beta}$ is the Kronecker symbol, and α and β run through the values 1, 2, and 3. The form of the dielectric tensor $\epsilon_{\alpha\beta}$ depends on the concrete properties of the medium. If we neglect collisions and the thermal motion of the particles, then the tensor $\epsilon_{\alpha\beta}$ is Hermitian and its form in a rectangular coordinate system with z axis directed along the external magnetic field $\mathbf{H}$ is

$$\varepsilon_{\alpha\beta} = \begin{Bmatrix} \varepsilon & ig & 0 \\ -ig & \varepsilon & 0 \\ 0 & 0 & \eta \end{Bmatrix},$$

$$\mathcal{L} = 1 - \sum_j \frac{\omega_{0j}^2}{\omega(\omega - \Omega_j)}, \quad \mathcal{R} = 1 - \sum_j \frac{\omega_{0j}^2}{\omega(\omega + \Omega_j)}, \quad \eta = 1 - \sum_j \frac{\omega_{0j}^2}{\omega^2},$$

$$\varepsilon = \frac{1}{2}(\mathcal{L} + \mathcal{R}), \quad g = \frac{1}{2}(\mathcal{L} - \mathcal{R}). \tag{2}$$

Here $\omega_{0j} = \sqrt{4\pi e_j^2 N_j / m_j}$ is the plasma frequency, $\Omega_j = e_j H/m_j c$ is the gyrofrequency, e_j, m_j and N_j are the charge, mass, and the concentration of particles of species j, and c is the speed of light. The summation is over all the species of particles making up the plasma.

A magnetoactive plasma is a dispersive anisotropic medium, i.e., n depends on ω and on the angle θ between $\mathbf{k}$ and $\mathbf{H}$. Two transverse waves of circular polarization propagate strictly along the external magnetic field ($\theta = 0$); the magnetic vector $\mathbf{h}$ of one wave rotates in the right-hand direction, and that of the other in the left-hand direction (when viewed along $\mathbf{H}$). We shall speak for brevity of $\mathcal{R}$ and $\mathcal{L}$ waves, as is customary in the geophysical literature. The square of the refractive index for these waves is equal to $n_+^2 = \mathcal{R}$ and $n_-^2 = \mathcal{L}$ respectively (see (2)). If the plasma consists of electrons and ions of only one species, then at $\theta = 0$ and $\omega \ll \Omega_e$ we have

$$n_\pm^2(\omega) = \frac{n_a^2}{1 \pm (\omega/\Omega_i)} + 1. \tag{3}$$

where $n_a = c/v_a$, $v_a = H/\sqrt{4\pi m_i N}$ is the Alfven velocity, $\Omega_{e,i}$ is the gyrofrequency of the electrons and ions, and N is the electron concentration. At still lower frequencies ($\omega \ll \Omega_i$), we have for the refractive index $n_+ \approx n_a$ and $n_- \approx n_a/|\cos\theta|$. In magnetohydrodynamics, these waves are known as the fast magnetosonic and Alfven waves[59]. If $\theta_a \neq 0$, the polarization of the hydromagnetic waves is almost linear (a strongly oblate ellipse). The magnetic-field perturbation vector $\mathbf{h}$ in the Alfven wave is perpendicular to the plane of the vectors $\mathbf{k}$ and $\mathbf{H}$; in the magnetosonic wave $\mathbf{h}$ is perpendicular to $\mathbf{k}$ and lies in the plane of $\mathbf{k}$ and $\mathbf{H}$.

Let us indicate the main limits of applicability of the presented formulas. The plasma pressure should

be much smaller than the magnetic pressure: $N(T_e + T_i) \ll H^2/8\pi$ ($T_{e,i}$—particle temperature). In the magnetosphere this condition is satisfied with a large margin[65]. For the $\mathcal{L}$ wave, formula (3) is valid when $|1 - \Omega_i/\omega|^{3/2} \ll v_{Ti}/v_a$, where $v_{Ti} = \sqrt{2T_i/m_i}$. In the magnetosphere, $v_a \sim 3 \times 10^7 - 5 \times 10^8$ cm/sec, and the thermal velocity of the ions changes from $v_{Ti} \sim 4 \times 10^4$ cm/sec in the ionosphere to $v_{Ti} \sim 3 \times 10^6$ cm/sec on the periphery of the magnetosphere. Thus, expression (3) for $n_+(\omega)$ is not valid only at frequencies directly adjacent to the ion gyrofrequency. The formula $n_- = n_a/|\cos\theta|$ is incorrect only in a narrow angle interval close to $\pi/2$.

The plasma next to the earth contains several types of ions with different charge/mass ratios. Up to altitudes on the order of 1000–2000 km, the plasma contains oxygen, nitrogen, helium, and hydrogen ions. At these altitudes, however, we have $\omega \ll \Omega_{O2}^+$ in the magnetic-pulsation band, and the fact that the plasma is a multicomponent one can be taken into account in elementary fashion by introducing a suitable expression for m_i in the formula for the Alfven velocity. With increasing distance from the earth, the concentration of the heavy ions decreases rapidly practically to zero. As to the He^+ ions, their presence was observed up to altitudes ~30,000 km[66] (at a relative concentration $\xi = N(He^+)/N \sim 0.01$). A formula for the refractive index of a plasma consisting of electrons, protons, and helium ions was obtained in[67,68]. The dispersion curves for a proton-helium plasma are shown in Fig. 13. We note that the presence of a small admixture of He^+ ions greatly influences the behavior of the dispersion curves only in the immediate vicinity of the gyrofrequency Ω_{He^+}.

In the geometrical-optics approximation, the direction of velocity of propagation of a wave packet is given by the group-velocity vector $\mathbf{v}_{gr} = \partial\omega/\partial\mathbf{k}$. The projection of $\mathbf{v}_{gr}$ on $\mathbf{k}$ is[6]

$$v_{gr} = \frac{c}{\frac{\partial\omega n}{\partial\omega}}, \qquad (4)$$

and the angle between $\mathbf{k}$ and $\mathbf{v}_{gr}$ is

$$\psi = \operatorname{arctg}\left\{-\frac{1}{n}\frac{\partial n}{\partial\theta}\right\}. \qquad (5)$$

Figure 14a shows the dependence of v_{gr} on ω for $\mathcal{L}$ waves at $\theta = 0$ and different values of ξ[69]. The group velocity decreases rapidly when ω approaches the gyrofrequencies. Figure 15 illustrates the effect of channeling of the $\mathcal{L}$ waves by an external magnetic field ($\xi = 0$)[70]. We see that the angle $\alpha = \theta - \psi$ between $\mathbf{v}_{gr}$ and H does not exceed 12.3° at all directions of the vector $\mathbf{k}$. In other words, a packet of $\mathcal{L}$ waves propagates almost exactly along the external magnetic field. For $\mathcal{R}$ waves, a similar magnetic-focusing effect occurs in the whistler band ($\Omega_i \ll \omega < \Omega_e$). In the band of interest to us, the $\mathcal{R}$ waves propagate isotropically ($\psi \ll 1$) with a group velocity on the order of the Alfven velocity.

Observations of pearls in conjugate points clearly indicate that the trajectories of the signals in the magnetosphere are the force lines of the geomagnetic field[18,71,72]. Since a special plasma distribution is necessary for the focusing of the $\mathcal{R}$ waves (see below), it is natural to assume that the pearls are packets of

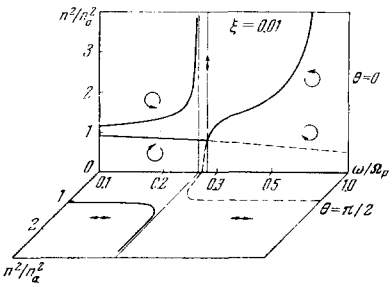

FIG. 13. Dispersion curves in a proton-helium plasma. The cases of longitudinal and transverse propagation are shown. The arrows designate the character of polarization of the waves.

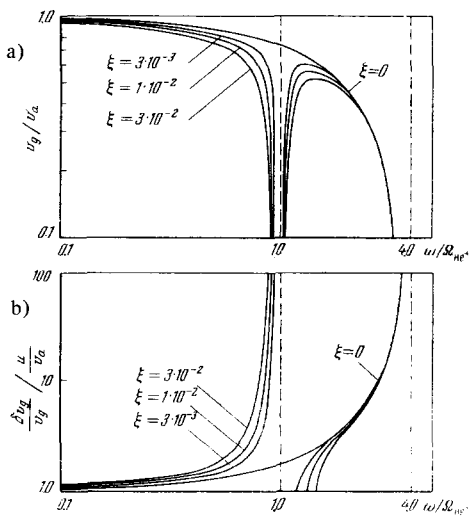

FIG. 14. Group velocity of $\mathcal{L}$ waves. a) Group velocity in a stationary plasma; b) correction due to the plasma motion.

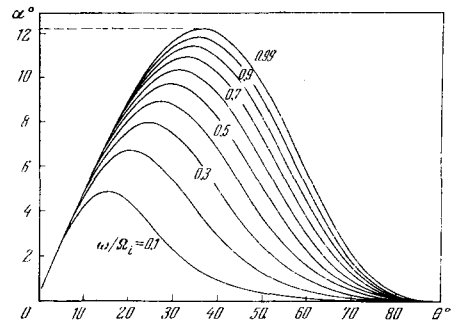

FIG. 15. Effect of magnetic focusing of $\mathcal{L}$ waves (see the text) [70].

$\mathcal{L}$ waves[71,72]. This makes it also possible to explain the inclination of the structure elements on the sonograms to the time axis (see Fig. 3). In fact, when a packet of $\mathcal{L}$ waves propagates upward along a force line, the carrier frequency a approaches the gyrofrequency of the ions, and the packets spread out as a result of dispersion. The low-frequency components lead the high-frequency components, so that a signal with rising tone is observed on the earth's surface. The reflection of the signal from the ionosphere at the conjugate points leads to the appearance of a series of pearls.

The repetition period of the pearls is

$$\tau(\omega) = 2\int \frac{dl}{|v_{rp}|}, \qquad (6)$$

where dl is the element of the trajectory r (of the force line), and the integral is taken between the conjugate points. In a spherical coordinate system, the equation of the force lines of the dipole field is given by

$$\frac{r}{r_e} = L\cos^2\varphi, \qquad (7)$$

where φ is the geomagnetic latitude, and L is the distance to the crest of the force line in units of the earth's radius $r_e = 6.4 \times 10^8$ cm. The magnetic field intensity along the force line with parameter L is

$$H = \frac{H_0}{L^3}\frac{\sqrt{1+3\sin^2\varphi}}{\cos^6\varphi}, \qquad (8)$$

where $H_0 = 0.31$ G is the geomagnetic field at the equator. The distribution of the plasma concentration can be specified, for example, in the form $N = N_0(r_e/r)^3$. Figure 16 shows the dynamic spectra of the $\mathscr{L}$ waves, calculated by means of formulas (3), (4), (6)—(8)[72]. To simplify the calculation, it was assumed that the signal is instantaneously emitted at the latitude φ_0.

Let us estimate the applicability of geometrical optics to the present case. We put $n \sim n_a$ in the well known condition $|1/n^2\, dn/dl\ c/\omega| \ll 1$. Then $d\ln n/dl < d\ln H/dl \sim 3l$, where l is the coordinate along the force line and is reckoned from the center of the magnetic dipole. If we recognize that the repetition period τ is of the order of magnitude of $\sim 6r_eL/v_a$, then the indicated condition can be written in the form $\tau f \gg 3r_eL/l$. Since $1 < l/r_e \lesssim 1.5L$ and $f\tau \sim 10^2$ (see Sec. 1.1), the use of geometrical optics is apparently justified.

Comparing the theoretical sonograms of the pearls with those observed experimentally, we can estimate the ratio of the carrier frequency ω to the gyrofrequency of the protons at the crest of the trajectory. The value of ω/Ω_p measured in this manner varies from case to case in the range ~ 0.3—0.7, and its average value is ~ 0.5[73-77]. Similar figures were obtained in[78] by an independent method. But this means that ω is larger than Ω_{He^+} at the crest of the trajectory[79,80]. Consequently, a packet of $\mathscr{L}$ waves propagating from one conjugate point to another can cross two non-transparency bands symmetrically located relative to the plane of the equator (see Fig. 13). The signal amplitude attenuation is of the order of[79] $(A\ (dB) \approx 5.4 \times 10^{11}[f^{2/3}\xi/v_a]$. At typical values $\xi \sim 10^{-2}$, $v_a \sim 10^8$ cm/sec and $f \sim 1$ Hz, the attenuation is quite large, $A \sim 54$ dB.

In order to reconcile the presence of He^+ ions in the magnetosphere with the results of the measurement of the ratio ω/Ω_p, it is necessary to conclude that the trajectory of the pearls is "combined" (Fig. 17)[77]. The signal propagates from the crest of the force line in the form of a packet of $\mathscr{L}$ waves. At the point of the trajectory where $\omega \approx \Omega_{He^+}$, inversion of the polarization takes place, and the signal finishes its further path towards the earth in the form of $\mathscr{H}$ waves propagating in a plasma column layer that is elongated along the force line. Since the dispersion effects occur principally in the crest part of the trajectory, the form of the dynamic spectra remains practically unchanged.

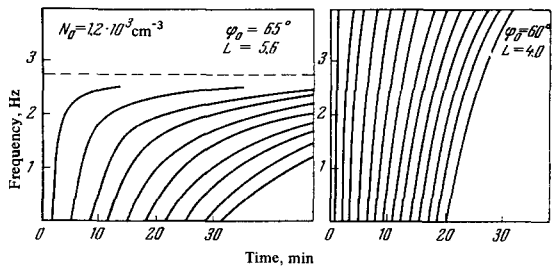

FIG. 16. Theoretical sonogram of pearls [72]. The dashed line on the last figure shows the value of the gyrofrequency of the protons at the crest of the force line.

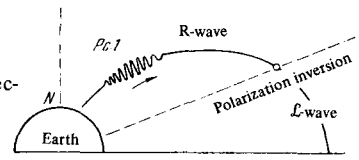

FIG. 17. "Combined" trajectory of pearl.

The condition under which the curvature of the rays resulting from the refraction of $\mathscr{H}$ waves in an inhomogeneous medium is equal to the curvature of the geomagnetic force lines is determined in[81]. In the frequency region $\omega < \Omega_i$, the magnetic focusing of the $\mathscr{H}$ waves is possible only if the plasma concentration decreases quite sharply in a direction perpendicular to the magnetic shell. A similar concentration gradient exists in the region of the so-called "knee" (or plasma pause[82,83]), the position of which varies in the interval $L \sim 4$—6, depending on the level of the magnetic activity. One cannot exclude the existence in the magnetosphere of other formations of the type of elongated plasma fibers, capable of channeling the $\mathscr{H}$ waves. However, in the region where the plasma-concentration gradients are abrupt, geometrical optics is not applicable and a more rigorous calculation is necessary to justify the hypothesis of combined pearl trajectory.

We shall not consider here other types of low-frequency waves that probably exist in the magnetosphere, since their identification with the pulsations observed on earth is still problematic. We point out, however, the slow magnetosonic waves that possibly contribute to the spectrum of the random pulsations in the aurora zone. The dispersion relation is of the form[63] $\omega = kv_s|\cos\theta|$, and the damping decrement is $\gamma \sim \sqrt{m_e/m_i}$. Here $v_s = \sqrt{T_e/m_i}$, and it is assumed that $T_e \gg T_i$, for otherwise the waves attenuate strongly. At $L \sim 7$ and $v_s \sim 5 \times 10^6$ cm/sec, the travel time of the wave packet from one conjugate point to the other is of the order of $\tau \sim 1$ hour. From the condition $\tau\gamma \lesssim 1$ we find that waves with a period $T \gtrsim 1$ min attenuate weakly.

So far we have spoken of propagation of waves in an immobile plasma. Under cosmic conditions, however, a moving plasma is a prevalent phenomenon. In interplanetary space, solar corpuscular streams are transported with large velocities. In the magnetosphere, there exists a complicated system of convective, drift, thermodiffusion, and similar plasma motions. Finally, the plasma is in motion relative to an electromagnetic-wave receiver mounted on a satellite or a rocket.

The distortion of the trajectory and the additional delay of the signals propagating in a moving plasma are small as a rule. One can therefore use the expression for the refractive index n' of a moving plasma, accurate to terms of first order in $\beta = u/c$[84]:

$$n' = n - \beta_z \left\{ \left(1 - n\frac{\partial\omega n}{\partial\omega}\right)\frac{\cos\gamma}{\cos\eta} - \frac{1}{n}\frac{\partial n}{\partial\cos\theta}\left(1 - \frac{\cos\gamma\cos\theta}{\cos\eta}\right)\right\}. \quad (9)$$

Here n is the refractive index of the plasma at rest, and if u is the plasma motion velocity, then $\beta_z = u_z/c$, $u_z = u\cos\eta$, and γ and η are the angles that u makes with the vectors **k** and **H** respectively. The group-velocity correction $\delta v_{gr} = |v'_{gr} - v_{gr}|$, calculated by means of formula (9), has a maximum in the gyrofrequency region (Fig. 14b). The experimentally observable features of wave propagation in a moving cosmic plasma are considered in[85,86].

2.2. Natural oscillations of the magnetosphere. In the calculation of the spectrum of the natural oscillations of the magnetosphere, one usually starts with the linearized system of equations of ideal magnetohydrodynamics[87]

$$\left.\begin{aligned} \frac{\partial\mathbf{h}}{\partial t} &= -c\,\mathrm{rot}\,\mathbf{E}, \quad \rho\frac{\partial\mathbf{v}}{\partial t} = \frac{1}{c}[\mathbf{jH}], \\ \mathbf{j} &= \frac{c}{4\pi}\mathrm{rot}\,\mathbf{h}, \qquad \mathbf{E} = -\frac{1}{c}[\mathbf{vH}]. \end{aligned}\right\} \quad (10)^*$$

where $\rho = Nm_i$ is the plasma density, **E**, **h**, **v**, and **j** are small perturbations of one order. In Eqs. (10), we have omitted the displacement current and the pressure gradient. In addition, we have neglected the Hall effect, the Joule dissipation, and effects of viscosity and thermal conductivity. The validity of the equations in this form for the description of oscillations of the magnetosphere is discussed in[87].

Differentiating the first equation of (10) with respect to time and eliminating the field **E** from this equation with the aid of the remaining equations, we obtain a wave equation for **h**:

$$\mathrm{rot}\{(4\pi\rho)^{-1}[\mathbf{H}[\mathbf{H}\,\mathrm{rot}\,\mathbf{h}]]\} - \frac{\partial^2\mathbf{h}}{\partial t^2} = 0. \quad (11)$$

Similarly we obtain an equation for **E**:

$$(4\pi\rho)^{-1}[\mathbf{H}[\mathbf{H}\,\mathrm{rot}\,\mathrm{rot}\,\mathbf{E}]] - \frac{\partial^2\mathbf{E}}{\partial t^2} = 0. \quad (12)$$

Equations (11) and (12) are equivalent, but one or the other turns out to be more convenient in the solution of concrete problems.

In a certain degree approximation we can regard the magnetosphere as actually symmetrical and seek solutions of the wave equation that depend on φ like $e^{im\varphi}$, where m = 0, 1, 2, ..., and φ (which must not be confused with the symbol for latitude) is the azimuth of the spherical coordinate system (r, ϑ, φ) with polar axis along the symmetry axis. The form of the wave equation greatly simplifies if the oscillations are also symmetrical (m = 0). For this case we have two uncoupled second-order differential equations[87]. One of them describes the so-called torsional oscillations

$$(r\sin\theta)(\mathbf{H}\nabla)\{(4\pi\rho)^{-1}(r\sin\theta)^{-2}(\mathbf{H}\nabla)(h_\varphi r\sin\theta)\} = -\frac{\partial^2 h_\varphi}{\partial t^2}, \quad (13)$$

and the other the polhode oscillations

$$\left[\frac{\partial^2}{\partial r^2} - \frac{\sin\theta}{r^2}\frac{\partial}{\partial\theta}\frac{1}{\sin\theta}\frac{\partial}{\partial\theta}\right]\chi = \frac{1}{v_A^2}\frac{\partial^2\chi}{\partial t^2}. \quad (14)$$

*$[\mathbf{jH}] \equiv \mathbf{j} \times \mathbf{H}$.

We have introduced here the symbol $\chi \equiv r\sin\theta E_\varphi$. Oscillations of this class are linearly polarized, and in the torsional oscillations $\mathbf{h} = (0, 0, h_\varphi)$ $\mathbf{E} = (E_r, E_\vartheta, 0)$, $\mathbf{v} = (0, 0, v)$, and in the polhode oscillations $\mathbf{h} = (h_r, h_\vartheta, 0)$, $\mathbf{E} = (0, 0, E_\varphi)$, and $\mathbf{v} = (v_r, v_\vartheta, 0)$.

When $m \neq 0$ the situation is much more complicated. A certain simplification again arises at very large azimuthal numbers[87,88] but none of these cases have been sufficiently investigated. Principal attention has been usually paid to Eqs. (13)–(14), since they can be easily solved by numerical methods.

The boundary condition for the torsional oscillations is specified on the earth's surface, and in view of the high conductivity of the earth's crest, it is given by

$$E_t(r = r_e) = 0, \quad (15)$$

where E_t is the horizontal projection of the electric vector. In other words, the surface impedance of the earth is assumed equal to zero*. In investigations of polhode oscillations, the boundary conditions must in general be specified on the earth's surface, on the outer surface of the magnetosphere, and generally speaking on other separation surfaces, for example on the surface of the plasmapause[92,93].

Equation (13) describes oscillations of magnetic shells, wherein the different shells oscillate independently of one another. To calculate the spectrum, a model of the magnetosphere is specified, and as a rule Eq. (13) is solved numerically subject to boundary condition (15)[94-96]. Figure 18 gives an idea of the so-calculated dependence of the period of the fundamental mode of torsional oscillations on the latitude of intersection of the magnetic shell with the earth's surface[94]. Curve 1 corresponds to the model of the magnetosphere with a higher average density than curve 2.

The torsional oscillations can be identified with geomagnetic pulsations whose period depends on the observation latitude (Sec. 1.3). The dashed line in Fig. 18 is drawn through experimental points known from the literature[45,56]. It is seen that at low latitudes the observations are in better agreement with curve 1, and at high latitudes with curve 2. Since the break occurs at a latitude $\varphi_0 \sim 60°$ ($L \sim 4$), it can be assumed that this effect is a reflection of the existence of the plasmapause. (The existence of the plasmapause was not taken into account in the calculation of 1 and 2.)

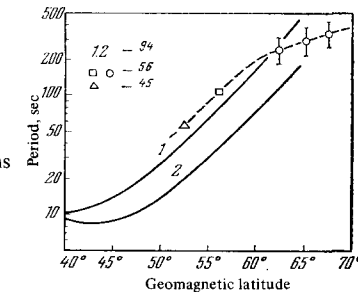

FIG. 18. Dependence of the period of the torsional oscillations on the geomagnetic latitude.

*In the micropulsation range, the impedance of the earth's surface is quite small, but of course differs from zero. The dependence of the impedance on the oscillation frequency is used for electromagnetic sounding of the earth in order to study the structure of its depth and to search for useful minerals [89-91].

Polhode oscillations described by Eq. (14) encompass the entire resonating region or else an appreciable part of it. The period of the oscillations depends little on the geomagnetic latitude. Analogous properties are possessed by pulsations of type Pc2—4. On this basis, they are assumed to be polhode oscillations of the magnetosphere[5-10,93,97]. In order of magnitude, the period of the oscillations is equal to $T \sim R/v_a$, where R is the characteristic dimension of the resonator, The distance from the boundary of the magnetosphere to the plasmapause is $R \sim 5\ r_e$, and the distance to the surface of the earth is $R \sim 10 r_e$. At $v_a \sim 10^8$ cm/sec, we obtain $T \sim 30$ sec and $T \sim 60$ sec, respectively.

There is no doubt that oscillations of the real magnetosphere can greatly differ from torsional or polhode oscillations. In this connection mention should be made of[88], where a direct variational method was used to estimate the natural frequencies of oscillations with large azimuthal numbers ($m \gg 1$). The authors of[88] assume that these are precisely the oscillations that are observed in the form of Pc2—4 pulsations.

2.3. Wave propagation in ionosphere layers. On approaching the earth, the density of the neutral atmosphere increases exponentially, and below a certain level the gas becomes only partially ionized. Below ~500 km, the collision of the electrons and ions with the neutral molecules begin to influence strongly the character of the propagation of the hydromagnetic waves; below ~150 km, this influence turns out to be decisive.

Another feature of wave propagation in this altitude region is connected with the sharp vertical inhomogeneity of the medium. This leads to formation of a hydromagnetic waveguide, in which the pulsations can propagate along the earth's surface.

The dielectric tensor $\epsilon_{\alpha\beta}$ of the partly ionized gas is obtained from (2) by formally replacing m_j by $m_j(1 + i\nu_j/\omega)$, where ν_j is the frequency of the collisions between the charged and neutral particles. No account is taken here of the electron-ion collisions or of the oscillations of the neutral gas. However, in the pulsation range, the influence of these factors is small. Knowing the expression for $\epsilon_{\alpha\beta}$ in terms of the plasma parameters, we can choose a concrete model of the ionosphere and attempt to solve in some manner the wave equation[60]

$$\Delta \mathbf{E} - \operatorname{grad}\operatorname{div}\mathbf{E} + \frac{\omega^2}{c^2}\mathbf{D} = 0, \qquad (16)$$

where $D_\alpha = \epsilon_{\alpha\beta} E\beta$. Even when account is taken of the fact that the ionosphere can be regarded as horizontally-layered, the problem of integrating (16) is in the general case very complicated, and it is necessary to confine oneself to an analysis of individual particular cases.

Many investigations have been devoted to the calculation of the propagation of vertically incident plane waves through the ionosphere[98-103]. Figure 19 gives an idea of the frequency dependence of the amplitude transmission coefficient of $\mathcal{R}$ and $\mathcal{L}$ waves through the daytime ionosphere (solid and dashed lines)[99]. The ionosphere is much more transparent at night than in the daytime.

In the case of oblique incidence, the $\mathcal{R}$ waves can become captured in the ionosphere layers. The existence of a hydromagnetic waveguide can be understood

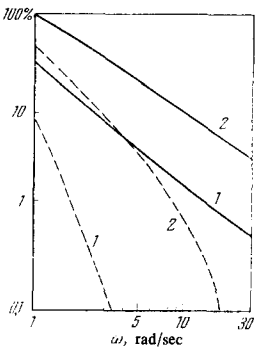

FIG. 19. Coefficient of transmission of hydromagnetic waves through the daytime ionosphere [99]. 1 – Maximal solar activity, 2 – minimal solar activity.

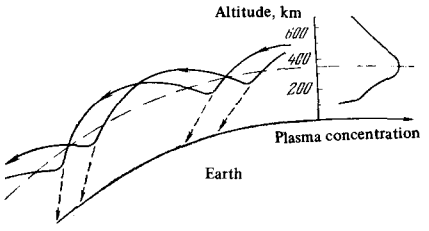

FIG. 20. Ionospheric wave guide.

from the following qualitative considerations. The vertical profile of the refractive index $n(z) \sim c/v_\alpha \sim \text{const} \cdot N^{1/2}(z)$ duplicates the profile of the plasma concentration, i.e., it has a maximum at an altitude of approximately 300 km. Since, as is known from geometrical optics, the rays bend towards the larger refractive index, the $\mathcal{R}$ waves will be concentrated towards the plane $z \approx 300$ km (Fig. 20)[104].

A rigorous theory of the hydromagnetic waveguide should include a description of the structure of the wave source and take into account the coupling of the modes, the sphericity, and the horizontal inhomogeneity of the ionosphere, etc. For perfectly clear reasons, no such complete theory has yet been developed. At the present time the principal efforts are directed at refining the qualitative picture. Simplified models are used to carry out numerical calculations of the critical frequency of the waveguide the phase and group velocity[105], the coefficient of waveguide attenuation[104], the wave polarization[106], etc. Methodological problems are being solved in the theory of wave propagation in inhomogeneous anisotropic media such as the ionosphere[107,108].

The fact that pearls with periods $T < 2$ sec are observed globally, and those with $T > 2$ sec more or less locally,[8] is indirect evidence of the existence of a waveguide with critical frequency ~0.5 Hz. The most direct proof of the waveguide propagation of pearls along ionospheric layers was provided by exact measurements of the time of arrival of individual signals at remote observation points. The obtained propagation velocity of pearls (several hundred km/sec) is close to the Alfven velocity in the F2 layer of the ionosphere[105].

3. Mechanisms of Pulsation Excitation

The cause of almost all types of geomagnetic pulsations is the instability of the cosmic plasma surround-

ing the earth*. Pulsations in the short-wave section of the spectrum (pearls, hydromagnetic hisses, oscillations with increasing frequency) are excited because of the kinetic instability of the distribution of the high-energy particles filling the magnetosphere. To the contrary, the long-wave pulsations (natural oscillations of the magnetosphere) are excited by instabilities of the hydrodynamic type, which occur, for example, when the solar wind flows around the magnetosphere.

The theory most thoroughly developed in the linear approximation is that of cyclotron instability of protons from the outer radiation belt[65,111-115]. The instability which many authors believe to be the cause of the pearls is due to the anisotropy of the velocity distribution of the high-energy protons. Progress was made also in the theory of excitation of waves on the surface of the geomagnetic cavity[87,88,123]. We present below the main results of these investigations. In passing, we discuss other generation mechanisms.

It should be noted that the development of the pulsation theory is only just begun, and many basic questions are not yet clear. This pertains primarily to the different nonlinear effects that occur in an unstable plasma. The waves growing inside the magnetosphere exert a noticeable influence on the distribution of the particles in the radiation belts[4,65]; strong turbulence develops on the periphery of the magnetosphere. The qualitative features of certain types of pulsations point to a hard regime of their excitation, i.e., the nature of such pulsations cannot be understood at all within the framework of the linear theory of instability. A thorough investigation of geomagnetic pulsations, on the one hand, and progress in plasma physics, on the other, will presumably lead in the nearest future to a deeper understanding of the mechanisms of excitation of low-frequency waves in the magnetosphere.

3.1. Kinetic instability. The resonance condition, under which effective energy exchange takes place between a wave and a particle, is given by[60]

$$\omega = s\Omega_j + ku\cos\theta, \quad s = 0, \pm 1, \pm 2, \ldots, \tag{17}$$

where Ω_j is the gyrofrequency and u is the projection of the particle velocity on the external magnetic field. The kinematic meaning of (17) is that in the coordinate system in which the Larmor center of the particle is immobile, the wave frequency is either equal to zero ($s = 0$) or else is a multiple of the particle gyrofrequency ($s \neq 0$). If $s = 0$, then (17) coincides with the condition for Cerenkov radiation; otherwise, (17) is the formula for the normal and anomalous Doppler effect for an oscillator of frequency Ω_j, if $s > 0$ or $s < 0$, respectively.

The resonant character of the instability of high-energy particles in the magnetosphere makes it possible to use expression (17) to estimate the spectrum of the frequencies of growing waves[116-122]. For example, in the case of resonance between protons and transverse waves traveling rigorously along the external magnetic field, we have[116]

$$\frac{u}{v_a} = \left(1 \pm \frac{\omega}{\Omega_p}\right)^{1/2}\left(1 - s\frac{\Omega_p}{\omega}\right). \tag{18}$$

This expression was obtained from (17) by eliminating $k = (\omega/c)n$ with the aid of (3). If $u \gg v_a$, then $\omega \approx \Omega_p(v_a/u)$. Near the maximum of the proton belt ($L \approx 4$), $\Omega_p \approx 47$ rad/sec, $v_a \approx 7 \times 10^7$ cm/sec, $u \approx 7 \times 10^8$ cm/sec, and $\omega \approx 4.7$ rad/sec.

In the approximation linear in the wave amplitude, the stability of a homogeneous plasma is investigated by analyzing the roots of the dispersion equation (1), in which suitable expressions are substituted for the components of the tensor $\epsilon_{\alpha\beta}$, which depend on the particle velocity distribution function[61-64]. (General formulas for $\epsilon_{\alpha\beta}$ are given, for example, in the review[62].) The magnetosphere is filled with a low-temperature plasma, which can be regarded as cold, and a small admixture of high-energy particles. Under these conditions, the dispersion equation for the hydromagnetic waves traveling along the force lines takes the form[111-115]

$$k^2 - \frac{\omega^2}{c^2}n_\pm^2(\omega) = -i\pi^2\frac{\Omega_p\omega_{0p}'^2}{c^2 k}\int_0^\infty v_\perp^2\,dv_\perp\left[\frac{kv_\perp}{\Omega_p}\frac{\partial f}{\partial v_z} \mp \frac{\partial f}{\partial v_\perp}\right]_{v_z = u}. \tag{19}$$

Here $\omega'_{0p} = \sqrt{4\pi e^2 N'/m_p}$, N' is the concentration, and $f(v_\perp, v_z)$ is the velocity distribution function of the high-energy protons. (The interaction with the electrons is ineffective in this case.) The resonance takes place at the first harmonic of the proton gyrofrequency: $u = (\omega \pm \Omega_p)/k$. The upper and lower signs pertain to $\mathscr{H}$ and $\mathscr{L}$ waves, respectively.

We put $\omega = \mathrm{Re}\,\omega > 0$ and $k = k' + ik''$. If $k'' > 0$, then the waves attenuate; but if $k'' < 0$, then they grow and the system is unstable. When $|k''/k'| \ll 1$, the real part of the wave number is determined by the cold plasma parameters: $k' = (\omega/c)n_\pm$, where $n_\pm$ is given by (3). The imaginary part depends on the concrete form of the distribution function of the high-energy protons. By choosing a two-temperature Maxwellian distribution

$$f(v_\perp, v_z) = \frac{m_p}{2\pi T_\perp}\sqrt{\frac{m_p}{2\pi T_\parallel}}\,e^{-\frac{m_p v_\perp^2}{2T_\perp}}\,e^{-\frac{m_p v_z^2}{2T_\parallel}}, \tag{20}$$

we obtain

$$k_\pm''(\omega) = \frac{1}{2}\sqrt{\frac{\pi}{2}}\frac{\omega}{u_\parallel}\left(\frac{\omega'_{0p}}{ck'_\pm}\right)^2\left[\frac{T_\perp}{T_\parallel} \mp \frac{\Omega_p}{\omega}\left(1 - \frac{T_\perp}{T_\parallel}\right)\right]\exp\left\{-\left[\frac{\omega - \Omega_p}{k'_\pm u_\parallel}\right]^2\right\}. \tag{21}$$

If the velocity distribution is isotropic ($T_\perp = T_\parallel$), then the waves attenuate. At "positive" anisotropy ($T_\perp > T_\parallel$), the $\mathscr{L}$ waves become intensified and the $\mathscr{H}$ waves attenuate, and vice versa in the case of "negative" anisotropy. Knowing k'' as a function of the parameters of the medium, it is possible to calculate in the geometrical-optics approximation the coefficient of amplification (attenuation) of a wave packet passing through a definite segment of path in the magnetosphere:

$$A(\omega) = \int_{l_1}^{l_2} k''(\omega, l)\,dl.$$

The described scheme is used, in various modifications, in the analysis of the instability of the proton belt[65,111-115]*.

*The only possible exception are magnetic fluctuations of the type shown in Fig. 4. They result from rapid variations of the jet stream flowing in the auroral zone at an altitude of approximately 120 km [12,109,110].

*The inhomogeneity of the magnetosphere is taken into account in [65] more correctly than in the present paper, and the formula obtained there for the gain is valid in the relativistic case.

In the proton belt, the transverse particle energy is larger than the longitudinal energy, i.e., positive anisotropy is obtained and $\mathcal{L}$ waves build up. On a given L-shell, the instability develops most rapidly near the equatorial plane. The dependence of the resonant frequency on L is given by the formula $\omega \approx 300/L^3$ rad/sec.

The instability has a convective character, i.e., the proton belt acts as an amplifier for gyromagnetic signals. Inasmuch, however, as the amplified signal returns to the system after being reflected from the ionosphere, positive feedback is produced and the belt can go over into the generation regime. The total amplification coefficient following two passes of the signal through the radiation belt is approximately equal to (see, for example,[10])

$$A(L)\,(\mathrm{dB}) \approx 10^{-5}\left(\frac{L}{10}\right)^4 I\Delta - 20\lg\left(\frac{1}{P}\right), \qquad (22)$$

where P is the coefficient of reflection from the ionosphere. At the maximum ($L \approx 4$), the flux of protons with energy $\gtrsim 100$ keV is of the order of[124] $I \approx 6 \times 10^7$ cm^{-2} sec^{-1}, and the degree of anisotropy of the temperatures $\Delta = (T_\perp/T_\parallel - 1) \approx 1$, from which it follows that generation occurs when $P \gtrsim 0.15$ (at a frequency ~0.7 Hz). The transition to the supercritical state is possible both when $I\Delta$ increases and when the wave-energy loss in the ionosphere decreases. Since the quantity $I\Delta$ is apparently not strongly dependent on the time of the day, and the absorption in the ionosphere is smaller during the night than in daytime, the most favorable for generation are the night hours.

With increasing growth of oscillation intensity, different nonlinear processes come into play. In[112], the scattering of protons by hydromagnetic waves is considered in the quasilinear approximation. The particles diffuse over the pitch angles, the degree of anisotropy decreases, and a certain fraction of the captured particles falls in the loss cone and leaves the boundaries of the geomagnetic trap. If the particle source is stationary, then the result is a stationary spectrum of hydromagnetic noise, a stationary flux of particles to the loss cone, and a stationary distribution of the captured particles. It is possible, incidentally, that the spectrum of the hydromagnetic noise in the proton belt is determined more readily by the interaction of the waves with one another than by the quasilinear diffusion[10].

It is doubtful whether pearls can be excited as a result of these processes, as is proposed in[65,111,113,115]. It is difficult to understand how an instability of the proton belt can lead to the formation of narrow-band signals that appear alternately in conjugate points. It is probable that hydromagnetic hisses, having no discrete structure (see Sec. 1.2), are excited in the proton belt[119].

The radiation of the proton belt is maximum on the L ~ 4 shell, whereas the trajectories of the pearls pass much higher[73-78], namely L ~ 5—8. A preliminary analysis of the isolated series of pearls has shown[125] that the proton flux at the maximum of the radiation belt is perfectly sufficient for the excitation of waves with the observed value of the gain in the range $\omega/\Omega_p \sim 0.1$. At the same time, similar values of ω/Ω_p were never really registered: the ratio of the frequency of the pearl to the gyrofrequency of the protons at the crest of the force line varies in the range ~0.3—0.7. The energy of the resonant protons amounts in this case to several keV (see Ch. III, Sec. 2). Moreover, according to the data of[125], the gain at the start of the series increases quite frequently with time, i.e., the growth of the amplitude is steeper than exponential. It can be proposed that the generation of the pearls occurs as a result of nonlinear instability with a hard regime[17]. In the generation region, the magnetosphere is stable against small perturbations, but wave packets of finite amplitude, occurring as a result of the fluctuations, become amplified and are observed in the form of pearls.

It is not easy to construct a concrete model of nonlinear instability. We call attention, however, to the following circumstance[17]. The fact that the carrier frequency of the pearl lies in the range $\Omega_{He^+} < \omega < \Omega_p$ does not seem accidental, for only in this case can the signals have a combined trajectory (see Fig. 17). In the linear approximation, the wave becomes amplified on the "$\mathcal{L}$ section" of the trajectory, and attenuates on the "$\mathcal{R}$ section" (see (21)). The total gain of the small-amplitude waves (when there are no captured particles) is smaller than zero, i.e., the system is stable. When a packet of waves of finite amplitude appears, capture of the resonant particles in the potential well of the wave becomes possible, the damping on the "$\mathcal{H}$ section" decreases, and the amplitude of the packet beings to grow. On the other hand, if a situation is produced in the magnetosphere wherein the $\mathcal{L}$ waves become amplified in the range $\omega < \Omega_{He^+}$, then the trajectories are simple, and hydromagnetic hisses become excited, but no pearls whatever.

We shall now discuss briefly the properties of pulsations with increasing frequency (see Fig. 6). In[43,126], one of the causes of the growth of the frequency is considered to be the change of the resonant properties of the ionosphere during the time of a magnetic storm. However, from this point of view it is difficult to explain the striking equality of the spectra at the conjugate points. Apparently, the change of frequency occurs directly in the generation region, which is located symmetrically with respect to the conjugate points, i.e., near the plane of the equator.

It is widely believed that depression of the geomagnetic field during the time of the principal phase of the storm is due to an annular current of protons with energy ~10 keV, drifting around the earth in the western direction[127]. It has been proposed in[114,128] that pulsations with increasing frequency are excited as a result of cyclotron instability of the protons of the annular current. Under the influence of the increasing hydromagnetic noise, the protons diffuse over the pitch angles and are spilled into the loss cone. The depression of the magnetic field decreases in the generation region, and the pulsation frequency increases. Observations, however, agree better with the point of view that the growth of the frequency is due to displacements of the resonant particles inside the magnetosphere under the influence of the large-scale electric field (see Ch. II, Sec. 2.3).

We mention, finally, an investigation[117] of the mechanism of generation of pulsed bursts of oscilla-

tion (see Fig. 5). The broad spectrum and the absence of dispersion indicate that the pulsations are excited at the lower ends of the force tubes, and the close connection between the appearance of bursts and the auroral activity makes it possible to identify the generation mechanism with instability of electron beams that penetrate into the auroral zone from the periphery of the nighttime magnetosphere.

3.2. Hydrodynamic Instability. The magnetosphere boundary over which the solar plasma flows is unstable against the buildup of surface waves[87,88]. The instability mechanism is similar to that leading to the appearance of wind waves on water.

In the simplest model, the magnetosphere boundary is flat and abrupt. On one side of the boundary (in the "magnetosphere") there is an immobile plasma with density ρ_1, and the magnetic field H_1 is parallel to the boundary. On the other side (in the "solar wind") a plasma with density ρ_2 moves parallel to the boundary with velocity U, and there is no magnetic field ($H_2 = 0$). Such a discontinuity in the parameters of the medium is classified in magnetohydrodynamics as tangential[59]. If the plasma is assumed to be incompressible, then the condition for the instability of the tangential discontinuity is given by

$$\mathbf{U}\mathbf{k} > \mathbf{H}_1\mathbf{k}\left(\frac{\rho_1+\rho_2}{4\pi\rho_1\rho_2}\right)^{1/2}.$$

The fastest to grow are surface waves traveling across the magnetic field[87].

It is assumed that a similar instability of the subsolar sections of the magnetosphere surface is responsible for the excitation of the daytime pulsations of the Pc2—4 type. However, the described model is overly simplified to attempt to obtain experimental confirmations of the hypothesis. In[88], account was taken of the curvature and finite thickness of the boundary, and mechanisms whereby the surface waves are transformed into natural oscillations of the magnetosphere were found. The transformation into oscillations of the Alfven type is effected in a linear manner (mode coupling), and the magnetosonic oscillations can be excited nonlinearly—with frequency doubling. There are known examples, when the period of the oscillations observed at the Lovozero high-latitude observatory was $T \approx 30$ sec[45]. It is perfectly probable that in these cases magnetosonic waves were observed in Borok and Alfven waves in Lovozero[87].

An analysis of effects connected with the cessation of Pc2—4 affords another possibility of verifying the hypothesis concerning the mechanism whereby oscillations of this type are generated. According to the results of[54], the Pc2—4 vanish when the ecliptic projection of the interplanetary magnetic field changes its orientation and becomes almost perpendicular to the sun-earth line (see Fig. 11). It must be assumed that we are dealing here with stabilization of the tangential discontinuity by the magnetic field H_2. For a flat model, the condition for the vanishing of the instability is[129]

$$\frac{H_1^2 H_2^2 \cos^2\psi}{H_1^2\sin^2\beta_1 - H_2^2\sin^2\beta_2} < \left(\frac{4\pi\rho_1\rho_2}{\rho_1-\rho_2}\right)U^2, \qquad (23)$$

where ψ is the angle between H_1 and H_2, and $\beta_{1,2}$ is the angle between $H_{1,2}$ and U. Figure 11 was constructed by using data on the interplanetary field behind the front of a frontal shock wave, i.e., in the unperturbed solar wind (see Fig. 9). On passing through the front, the magnetic force lines are refracted and wrap themselves around the magnetosphere surface in a complicated manner[130]. It is therefore difficult to analyze the available experimental data quantitatively on the basis of the formula of[23]. It is seen, however, that the inequality (23) is quite sensitive to changes of the orientation ψ of the field H_2.

On the surface of the magnetosphere, there is satisfied a balance condition of the type

$$\frac{H_1^2}{4\pi} \approx \rho_2 U^2, \qquad (24)$$

from which follows an approximate expression for the radius of the magnetosphere[127]

$$R \approx \left(\frac{H_0^2}{4\pi\rho_2 U^2}\right)^{1/6}. \qquad (25)$$

When the dynamic pressure of the solar wind decreases rapidly, R increases, and a negative magnetic pulse si$^-$ is observed on the earth's surface, behind which the Pc2—4 sometimes vanish. It is shown in[31] that the termination of the pulsations occurs only when R after the si$^-$ exceeds a certain critical value. (The method of estimating R from data obtained on the earth's surface will be described in the next chapter.) Qualitatively, this result also agrees with the notions concerning the stabilization of the boundary of the magnetosphere by the interplanetary magnetic field. In fact, by combining (23)—(25) we obtain the stabilization condition in the form $R \geq R_{cr}$, where

$$R_{cr} \sim \left\{\frac{\sin^2\beta_1}{\sin^2\psi}\left(\frac{H_0}{H_2}\right)^2 \Big/ \left[\left(1-\frac{\rho_2}{\rho_1}\right) - \frac{\sin^2\beta_2}{\sin^2\psi}\right]\right\}^{1/6}.$$

The mechanism of exciting the trains of the Pi2 oscillations, which are typical of the nighttime hemisphere, has a different nature. It is customary to assume that the Pi2 are reflections of the sporadic activity of the geomagnetic tail. No theory of the processes occurring in the tail has yet been developed, so that only qualitative opinions can be expressed with regards to the mechanism of Pi2 generation. Undoubtedly, an analysis of Pi (and of the closely related impulsive Pi1 bursts) will afford in the future a better understanding of certain aspects of these processes.

An opinion has been advanced that the tail of the magnetosphere is in a metastable state[132-135]. Under the influence of the inhomogeneities of the solar wind, part of the magnetic energy stored in the tail is released and is consumed in particle acceleration, excitation of the natural oscillations of the magnetosphere, etc. A major role in these processes is assigned to a neutral layer that divides the tail into two halves with oppositely directed force lines (Fig. 21). It is assumed that as a result of the instability stimulated by the change of the interplanetary conditions, a rejoining (spill-through) of the force lines through the neutral layer takes place, and the equilibrium of the tail is disturbed.

Without stopping in detail on the general analysis of these processes, which is a separate problem outside the scope of the present review, let us discuss one interesting feature of the pulsed Pi1 bursts, namely their periodicity.

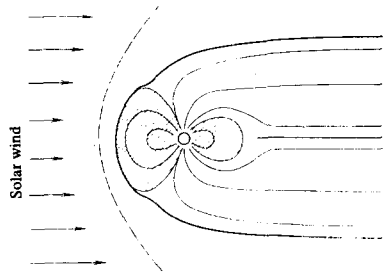

FIG. 21. Schematic section of the magnetosphere in the plane of the noontime meridian.

The repetition period τ of the bursts is of the order of magnitude of the travel time of a solitary pulse (or a weak shock wave) from the neutral layer to the lateral surface of the tail and back. Indeed,

$$\tau \approx \frac{a\sqrt{16\pi m_i N}}{MH}, \qquad (26)$$

where a is the radius of the tail, H and N are the unperturbed magnetic field and the concentration of the plasma in the tail. The Mach number for the solitary wave is $1 \leq M < 2$.[136]. At the typical values $a \approx 20$ earth radii, $H \approx 20\,\gamma$, and $N \approx 1$ cm^{-3}, we have $\tau \approx 5-10$ min, which is in full agreement with the observed repetition period of the bursts.

It is probable that the periodic bursts of pulsations are a remote after effect of a shock collapse of the magnetosphere tail[137]. During the spill-over of the force lines through the neutral layer, a pair of shock waves (or solitary pulses) is generated; this pair diverges towards the periphery of the tail. After reflection from the lateral surface of the tail, the waves travel opposite to each other. The collision of the waves near the neutral layer stimulates the first rejoining. Regeneration of the shock waves leads to multiple repetition of the effect.

III. DIAGNOSTICS OF THE MAGNETOSPHERE AND OF THE INTERPLANETARY MEDIUM

Sounding a plasma with electromagnetic waves is the classical method of measuring its parameters—density, temperature, ion composition, etc. By now, there is a well developed extensive arsenal of land-based and satellite methods of electromagnetic sounding of plasma in the outer-space vicinity of the earth. It is convenient to subdivide the methods into high-frequency and low-frequency (see Fig. 1). High-frequency waves are used in ionospheric sounding of the plasma concentration below the level of the maximum of the F2 layer. In the high-frequency band one uses powerful radars, which make it possible to investigate the plasma parameters above the principal maximum, by means of the method of inverse incoherent wave scattering. High-frequency waves are also used to measure plasma parameters by means of the Doppler frequency shift of a radio transmitter mounted on a satellite, by means of the Faraday rotation of the polarization plane, etc.[138]

Thus, in high-frequency sounding one uses artificial electromagnetic fields. At the same time, undisputed practical interest attaches to methods which make use of "gratis" electromagnetic radiation of natural origin, such as, for example, the VLF radiation and geomagnetic pulsations. The success attained in the use of whistlers for the diagnostics of plasma concentration in the magnetosphere is well known. Since 1953, the dawn of outer-space research, when the first correct estimate of the electron concentration at high altitudes was made[139], whistlers and others VLF radiations have won a permanent place in the arsenal of electromagnetic methods of sounding the magnetosphere. The use of geomagnetic pulsations for diagnostic purposes ("hydromagnetic sounding") is a natural continuation of this group of investigations[10]. Methods of magnetosphere research using data of pulsations and VLF radiation are similar to each other in many respects. At the same time, observations of pulsations make it possible, for example, to diagnose such an important parameter as the position of the magnetosphere boundary. There are no land-based methods whatever for the determination of this parameter.

1. Concentration of Cold Plasma

1.1. Diagnostics of plasma concentration by using the dispersion of pearls. It follows from the theory of pearl propagation that the dispersion of the signals increases the closer the carrier frequency is to the gyrofrequency of the ions at the crest of the trajectory, and the higher the plasma concentration. This circumstance makes it possible to use dispersion measurements of pearls to estimate the plasma concentration near the crests of force lines[73-77].

The fundamental formula in diagnostics theory is

$$\tau(\omega) = \frac{1}{c}\int_{(l)} n_{gr}(\omega, l)\, dl, \qquad (27)$$

which gives the frequency dependence of the signal repetition period. It is usually assumed that the plasma consists of electrons and ions of the same kind (protons), in which a transverse wave of left-hand polarization propagates strictly along the external magnetic field:

$$n = \frac{\omega_{0p}}{|(\Omega_p - \omega)\,\Omega_p|^{1/2}}. \qquad (28)$$

In this case the group refractive index $n_{gr} = \partial\omega n/\partial\omega$ is equal to

$$n_{gr} = \frac{\omega_{0p}\,[(\Omega_p - \omega/2)]}{\Omega_p^{1/2}(\Omega_p - \omega)^{3/2}}. \qquad (29)$$

Here $\omega_{0p} = \sqrt{4\pi e^2 N(l)/m_p}$, and $N(l)$ is the distribution of the plasma concentration along the force line. The problem consists of finding the magnitude of the concentration at the crest of the force line, assuming the function $\tau(\omega)$ to be known from experiment.

The main difficulty of the diagnostics consists in the following. The spectrum of the pearl is quite narrow, so that when the experimental function $\tau(\omega)$ is expanded in a series one can be assured that only the first two terms are reliable—the repetition period τ at the carrier frequency, and the first derivative $d\tau/d\omega$ of the repetition period with respect to the frequency. Therefore dispersion measurements make it possible to determine not more than two unknown

parameters. Yet the form of the function $\tau(\omega)$ depends, generally speaking, on the character of the plasma distribution $N(l)$ along the entire trajectory. Moreover, owing to the existence of a hydromagnetic waveguide, the signal can traverse a tremendous path along the earth's surface before it is registered. Therefore the position of the point of observation gives practically no information concerning the coordinates of the signal trajectory in the magnetosphere. The trajectory parameter L, contained in expressions (27)–(29), should be obtained from dispersion measurements.

In spite of all this, diagnostics is possible because of a fortunate combination of circumstances: the derivative $(\omega/\tau)d\tau/d\omega$ is a "universal" function of the ratio ω/Ω_p in the sense that its form depends little on the latitude of the intersection of the trajectory with the earth's surface, or on the character of the positive distribution along the trajectory*. This can be verified by calculating the group delay time $\tau(\omega)$ for a broad class of magnetosphere models[75,76]. Physically this means, on the other hand, that the main contribution to the dispersion is made by the near-equatorial section of the trajectory, on which the difference $(\Omega_p - \omega)$ is minimal. It is perfectly understandable that in this respect τ/τ_0 is also a "universal" function of the same argument (τ_0—repetition period of a packet of Alfven waves $(\omega \to 0)$).

The universal dispersion curves are shown in Fig. 22, 1. Analyzing the sonogram of the pearls, we first obtain $(\omega/\tau)d\tau/d\omega$. The plot is used to determine Ω_p, and consequently also the coordinate L of the trajectory. Knowing L, ω/Ω_p, and τ we can estimate the plasma concentration N at the crest of the trajectory. The results of such measurements are shown in Fig. 23[73,76].

When speaking of pearl propagation, we have noted that the presence of helium ions in the magnetosphere apparently causes the signal trajectory to become combined. If this hypothesis is true, then the diagnostics procedure described above requires a certain correction[77]. Figure 22, 2 shows the universal dispersion functions plotted with allowance for the fact that the pearls propagate along combined trajectories. When $\omega \gtrsim 0.5\Omega_p$, plots 1 and 2 differ little from each other, but at higher values of the ratio ω/Ω_p the coordinates L obtained with the aid of curves 1 are somewhat overestimated, and the concentration N is underestimated.

1.2. Diagnostics of plasma concentration using the spectrum of the torsional oscillations. The spectrum of the natural oscillations of the magnetosphere depends on the spatial distributions of the plasma and of the magnetic field. Since the structure of the geomagnetic field is known relatively well data obtained by observing the spectrum of the natural frequencies can be used to estimate the plasma concentration at large altitudes. Highly interesting from this point of view are the torsional oscillations. Different sections of their spectrum are formed in different regions of the magnetosphere. This makes it possible, in principle, to reconstruct from the known spectrum not only the

*Here and henceforth Ω_p is the proton gyrofrequency at the crest of the force line.

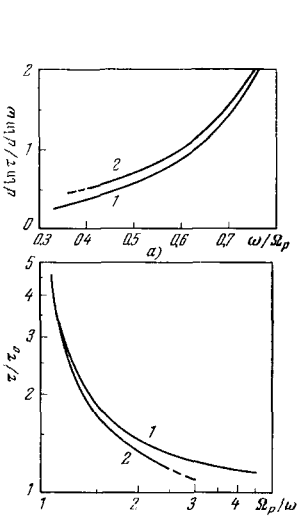

FIG. 22.

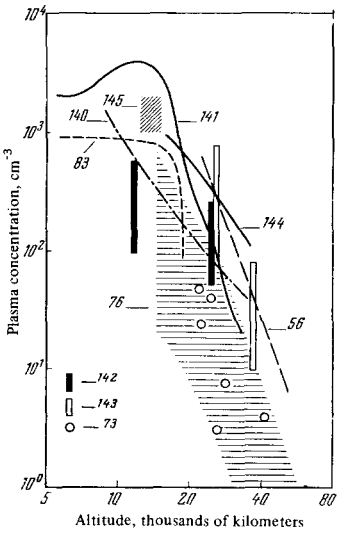

FIG. 23.

FIG. 22. "Universal" dispersion functions.

FIG. 23. Profiles of plasma concentration in the plane of the geomagnetic equator.

integral parameters of the plasma distribution, but also the local parameters[56 140-143].

The starting point in the analysis is Eq. (13) for the torsional oscillations of the magnetosphere. Let the equation of the force line have the form $\vartheta = \vartheta(r, r_0)$, where r_0 is the distance from the earth's centers to the crest of the line. By making the change of variables $\psi = h_\varphi r \sin\vartheta$, $F_1 = (r\sin\vartheta)^2 F$, $F_2 = (r\sin\vartheta)^{-2} F$, $F = H[1 + (r\,d\vartheta/dr)^2]^{-1/2}$, Eq. (13) is transformed into the more convenient form[141]

$$-\frac{F_1}{4\pi}\frac{d}{dr}\left(\frac{F_2}{\rho}\right)\frac{d\psi}{dr} = \omega^2\psi. \tag{30}$$

The boundary condition takes the form

$$\frac{d\psi}{dr}\Big|_{r=r_e} = 0. \tag{31}$$

The coefficients F_1 and F_2 are expressed in terms of the magnetic field, which can be regarded as potential inside the magnetosphere. Retaining the two principal terms in the Gaussian distribution, we get[90]

$$H_r = \left\{2H_0\left(\frac{r_e}{r}\right)^3 - H_1\right\}\cos\vartheta,$$
$$H_\vartheta = \left\{H_0\left(\frac{r_e}{r}\right)^3 - H_1\right\}\sin\vartheta. \tag{32}$$

The diagnostics consists of solving the inverse Sturm-Liouville problem for the torsional oscillations of the magnetosphere, namely it is required to determine ρ from the known spectrum of the natural oscillations. In view of the peculiar character of the problem, it is impossible to employ rigorous solutions of Eq. (30), which can be constructed for several concrete forms of $\rho(r)$. Therefore the use of approximate methods is practically unavoidable in any attempt at analytically solving the problem. For example, in the WKB approximation, the eigenvalues of Eq. (30) subject to the boundary condition (31) are determined by the relation

$$\int_{r_a}^{r_0}\frac{r^3\sqrt{\rho(r)}\,dr}{\sqrt{r_0 - r}}\{1 + \Phi(r, r_0)\} = \frac{r_e^3 H_{0s}\sqrt{\pi}}{2r_0^{1/2}\omega_s(r_0)}. \tag{33}$$

in which s = 1, 2, ... is the number of the harmonic, and $\Phi(r, r_0)$ is a small correction that takes into account the fact that the magnetic field is not of the dipole type.

We are interested in the question of reconstructing the form of the function $\rho(r)$ from the function $\omega_s(r_0)$, which is assumed known from experiment. From the mathematical point of view the problem reduces to solving the integral equation (33), in which $\rho(r)$ is regarded as an unknown function. Expression (33) is an integral equation of the Abel type, and it can be easily solved by successive approximations. In the first approximation we have[141]

$$\sqrt{N(r)} = \frac{H_0 s}{4\pi^{3/2} m_i^{1/2}} \left(\frac{r_e}{r}\right)^3 \left[1 + \frac{1}{2}\left(\frac{r}{r_m}\right)^3\right] \int_{r_e}^{r} \left(\frac{dT_s}{dr_0} - \frac{T_s}{2r_0}\right) \frac{dr_0}{\sqrt{r_0(r-r_0)}}. \quad (34)$$

Here

$$|r_m/r_e|^3 = |2H_0/H_1| \gg 1, \; T_s = 2\pi/\omega_s.$$

To calculate the concentration N at a distance r from the earth's center, it is necessary to know the form of the function $T(r_0)$ in the interval from r_e to r. Yet the latitudinal dependence of the period of the pulsations, which presumably are torsional oscillations, is given by $T(r_0)$ only in the interval $r_0 \sim (3.5-8)r_e$. However, at altitudes up to ~5000 km, the distribution of the plasma concentration is in itself well known from satellite and radar measurements[138]. The $T(r_0)$ spectrum in the interval $r_0 \sim (1-2)r_e$ can therefore be calculated theoretically, and interpolation is possible in the interval $r_0 \sim (2-3.5)r_e$ it is possible to interpolate it.

The described diagnostic method makes it possible to obtain the equatorial profile of the concentration N(r) without any a priori assumptions concerning its form. This was accomplished at the expense of a number of simplifications, the strongest of which is the use of the WKB solutions of Eq. (30). It can be shown, by using the fact that the eigenfunctions are extremal, that the calculation based on formula (34) yields the upper bound of the plasma concentration in the magnetosphere[10]. In principle, the accuracy of the results is monitored by the degree to which the observed spectrum $T_s(r_0 = \text{const})$ is not equidistant. We note that non-equidistance of the spectrum (if we succeed in measuring it) will in itself serve as additional information for the refinement of the parameters of the distribution N(r).

Of course, the inverse problem can be solved also by numerical methods. One usually seeks a solution of the corresponding direct problem at a specified hypothesis concerning the structure of the medium. A suitable approximation of the geomagnetic field is chosen, the distribution of the plasma concentration is described by means of a certain set of trial functions, and the spectrum of the torsional oscillations is calculated. Further, the parameters of the model are chosen in such a way that the theoretical and experimental spectra are as close as possible to each other. In[140], the vertical profile of the plasma density was sought in the class of functions of the type $\rho(r) = \alpha e^{\beta/r}$, where α and β are parameters to be determined, but the oscillation spectrum was calculated in the WKB approximation. A numerical solution of (30) for diagnostic purposes was undertaken in[142,143].

Some preliminary results of the determination of the plasma concentration in the magnetosphere are shown in Fig. 23. The vertical profiles in the plane of the geomagnetic equator were constructed by various methods on the basis of various data pertaining to different levels of the magnetic disturbances. This apparently explains the large scatter in the values of the concentration. Incidentally, the results obtained, for example, with the aid of satellites (curves[83,144,145] on Fig. 23) are subject to no less a scatter.

A method of estimating the plasma concentration in the geomagnetic tail from data on the repetition period of impulsive oscillation bursts is indicated in[137] (Fig. 5). To this end, it is necessary to eliminate the uncertainties of a and H from formula (26). The magnetic field is transferred to the tail from the polar caps and can be estimated from the latitude of the southern boundary of the aurora zone[146]. The radius of the tail is connected in some manner with the position of the subsolar point of the magnetosphere boundary, which is determined from the period of Pc2–4[52]. There still remains the uncertainty in the coupling coefficients, and one can speak only of the order of magnitude of the measured quantity. It is probable that the method will make it possible to study the time variation of the plasma concentration in the tail.

2. High-energy Particles

2.1. Energy of resonant protons. Let us estimate the energies of the protons responsible for the excitation of the pearls. The method with which it is possible to connect the observed spectrum of the growing waves with the longitudinal energy of the resonant particles is based on an analysis of relation (17). Assuming that the pearls are excited as a result of cyclotron instability, we choose the lower sign in (18) and put s = +1:

$$\mathcal{E}_p = \mathcal{E}_m \left(\frac{\Omega_p}{\omega}\right)^2 \left(1 - \frac{\omega}{\Omega_p}\right)^3. \quad (35)$$

Here $\mathcal{E}_p = m_p u^2/2$, and $\mathcal{E}_m = A^2/8$ N is the density of the magnetic energy per particle of the cold plasma in the generation region. To estimate $\mathcal{E}_p$ it is necessary to know ω/Ω_p at the crest of the trajectory or, which is practically the same, the trajectory parameter L. Dispersion measurements give a value $\omega/\Omega_p \sim 0.5$. At a frequency f ~ 1 Hz, the typical parameter of the trajectory will be L ~ 6, $\mathcal{E}_m \sim 4$ keV, and consequently $\mathcal{E}_p \sim 2$ keV.

In view of the importance of this entire problem, we call attention to another possibility of estimating L and $\mathcal{E}_p$, which arises in certain special cases[10,147]. If the magnetosphere is suddenly compressed, the radiation spectrum should change. In fact, upon compression of the magnetosphere, the gyrofrequency increases both as a result of the strengthening of the geomagnetic field and as a result of the radial drift of the radiator to the interior of the magnetosphere. Further, a change takes place in the longitudinal velocity of the radiators (betatron acceleration, change of the pitch angles). Finally, changes take place in the surrounding-plasma parameters on which the magnitude of the wave vector

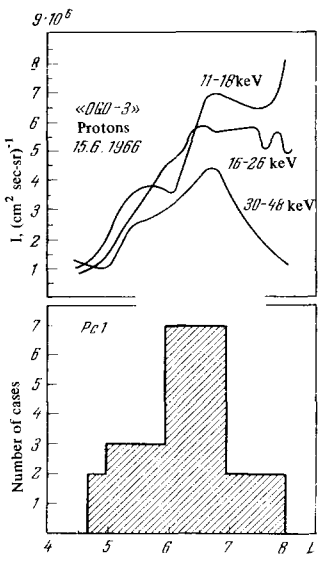

FIG. 24. Distribution of pearls over the L shells. In the upper part of the figure are shown the profiles of fluxes of protons with various energies.

depends. It turns out that the resultant change $\Delta\omega$ of the radiation frequency at a specified value of the magnetosphere deformation is a function of only one variable, the ratio ω/Ω_p. The deformation of the magnetosphere is determined from the magnitude of the sudden geomagnetic-field pulse ΔH registered by an equatorial observatory.

By measuring ω, $\Delta\omega$, and ΔH, we get L by means of the formula[10,147]

$$L \approx 5.7 \left(\frac{\Delta\omega}{\omega}\frac{10^2}{\Delta H_\gamma}\right)^{1/3}. \quad (36)$$

Typical values of $\Delta\omega/\omega \approx 0.2$ and $\Delta H \approx 20\ \gamma$ yield an estimate $L \approx 5.7$ and $\mathcal{E}_p \approx 3$ keV. This method was used in[78] to analyze 14 series of pearls, during the time of which sudden si pulses and sudden starts of magnetic storms ssc were observed. The distribution of the pearls over the L-shells is shown in Fig. 24. The scatter of the obtained values of the energy is quite large: $\mathcal{E}_p \sim 0.5$–15 keV. For comparison, in the upper part of Fig. 24 are shown the profiles of the flux of protons of different energies as obtained by the satellite "OOG-3"[148].

2.2. Distribution function of high-energy protons. If it is recognized that an exceedingly broad class of distribution functions f(v) can be realized in a collisionless plasma, then the problem of reconstructing f(v) in a magnetosphere from land-based data is quite hopeless. However, if the distribution of the particles is unstable against buildup of hydromagnetic waves and the general form of f(v) is known approximately from some indirect considerations, then we can attempt to refine the distribution parameters by using data on pulsations excited as a result of the instability.

In order to present more clearly the idea of the corresponding methods, it will be useful to digress somewhat and consider the problem of diagnostics as a whole. The general scheme of magnetic sounding consists in the following. One determines first the connection between the complex refractive index n and the local parameters of the medium. A connection is then sought between the observable parameters of the electromagnetic field and the distribution of n along the paths of wave propagation. Finally, an attempt is made to construct the spatial distribution of the investigated parameter of the medium from the observational data on the electromagnetic field. The last stage reduces in the general case to a solution of a certain integral equation.

The possibility of formulating the diagnostics problem as a problem involving the solution of an integral equation does not mean, of course, that this must always be done. Owing to the incompleteness and the inaccuracy of the experimental data, a rigorous solution of the inverse problem is in many cases practically unrealizable, so that it becomes necessary to confine oneself only to estimates of the parameters, by starting from simple heuristic considerations. It is precisely such a simplified variant that was used in the estimate of the concentration of the plasma from the dispersion of the pearls and in the estimate of the energy of the resonant particles from the spectrum of the observed radiations. In the former case, a study was made of the real part Re $n(\omega)$ of the refractive index, which is determined by the parameters of the cold plasma under the assumption that the attenuation (buildup) of the waves is weak. To the contrary, in the latter case one investigates implicitly the imaginary part Im $n(\omega)$ of the refractive index, which depends on the distribution function of a small admixture of high-energy particles. In this case one uses essentially only the fact that the excitation of the pearls is due to the instability that develops in the frequency region where Im $n(\omega) < 0$. The next step is a more detailed investigation of the function Im $n(\omega)$ from observation data on growing waves.

From the growth rate of the pearl amplitude at one of the conjugate points, one can attempt to estimate the gain after two passes of the signals through the magnetosphere: $A^* = 20 \log[h(t+\tau)/h(t)]$. The initial data obtained in this manner must be compared with the theoretical values of the gain, calculated under various assumptions concerning the parameters of the distribution function of the high-energy protons*.

The realization of such a program is a complicated and subtle problem, which requires further experimental research for its final solution. A preliminary analysis of the coefficients A^* of isolated series of pearls is contained in[125]. The maximum gain A_1^* at the start of the series and the attenuation coefficient A_2^* at the end of each series of pearls was estimated from the envelope of the signal amplitude (Fig. 25). By way of an illustration, let us estimate $I\Delta$ from formula (22), using the data of Fig. 25. A_1^* should be of the order of A, and $A_2^* \sim -20 \log(1/P)$. Recognizing that $A_1^* - A_2^* \sim 10$ dB, we get $I\Delta \sim 4 \times 10^7$ cm^{-2} sec^{-1} and $I\Delta \sim 4 \times 10^6$ cm^{-2} sec^{-1} at $L \sim 4$ and ~ 7, respectively.

2.3. Nonstationary processes in a geomagnetic trap.

*In cases of practical interest, the distribution function f(v) is characterized by three parameters: the particle concentration, the slope of the energy spectrum, and the degree of anisotropy of the distribution with respect to the pitch angles α. The gain in the frequency region $\omega \ll \Omega_p$ was obtained in [65] for a function in the form $f = \text{const} \cdot v^{-2\nu} \sin^{2\mu}\alpha$. A series of plots of $A(\omega)$, which is convenient for the comparison at different values of ν and μ, is contained in [113].

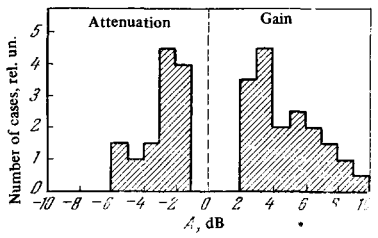

FIG. 25. Distribution of the gain and attenuation coefficients of pearls.

tric field on the periphery of the night time magnetosphere[149-151].

3. Boundary of the Magnetosphere

3.1. Daytime boundary of the magnetosphere. It is shown in[13,52] that the Pc2–4 pulsations are an effective indicator that makes it possible to trace continuously the position of the daytime boundary of the magnetosphere. The idea of the method consists in the fact that, since Pc2–4 are natural oscillations their period T should depend on the dimensions R of the

Table II

Data	Data on pulsations			Data on the radiation belt					
				Outer boundary of belt			Flux ($\mathcal{E}_e \geqslant 100$ keV), sec^{-1}		
	Start UT	End UT	Final frequency, Hz	Start	End	δL	Start	End	δI
31.01 1964	11.54	12.35	0.80	6.0	5.0	1.0	$3.5 \cdot 10^2$	$2 \cdot 10^2$	$1 \cdot 10^2$
12.02 1964	13 59	14.45	0.80	6.5	5.3	1.2	$5 \cdot 10^2$	$4 \cdot 10^2$	$1 \cdot 10^2$
20.02 1964	15.52	16.26	0.80	6.0	5.0	1.0	$7 \cdot 10^2$	$5 \cdot 10^2$	$2 \cdot 10^2$
20.02 1964	17.48	19.22	1.55	6.0	4,65	1.5	$7 \cdot 10^2$	$2 \cdot 10^2$	$5 \cdot 10^2$
17.07 1964	17,13	18.23	1.55	6.5	5	1.5	$6 \cdot 10^2$	$2 \cdot 10^2$	$1 \cdot 10^2$

During the time of magnetic storm, a complicated picture of electrodynamic and kinetic phenomena develops in the space near the earth in a definite sequence Some of them are accompanied by low-frequency radiation, which can be likened to the whistling and howling of winds during the time of storms in the atmosphere.

Let us discuss the information that can be extracted concerning the dynamics of the magnetosphere from observations of pulsations of increasing frequency, which arise during the most active phase of the storm (see Fig 6). The very fact that the frequency increases is a reflection of the nonstationary character of the geomagnetic trap. This point of view is confirmed by a large number of comparisons of the spectra of the pulsations with changes of the radiation-belt parameters. An interesting connection has been observed between the displacement of the outer boundary of the belt and the limiting frequency of the pulsations (see Fig. 7 and Table II[9,11]).

Let us assume that the growth of the pulsation frequency is a result of transfer of resonant particles across the L shells under the influence of a large-scale electric field*. If we assume the cyclotron mechanism of pulsation excitation, then we can obtain an estimating formula which relates the field component E_φ (western direction) with the rate of frequency growth[152]:

$$E_\varphi \approx -\frac{r_e m_p}{3e}\left(\frac{\Omega_p^{(0)}}{\omega}\right)^{1/3}\frac{d\omega}{dt}. \qquad (37)$$

Here $\Omega_p^{(0)} = 3 \times 10^3$ rad/sec. The average frequency is ~ 6 rad/sec and the frequency drift is $\dot{\omega} \sim 5 \times 10^{-3}$ rad/sec^2, hence $E_\varphi \sim 10^{-5}$ V/cm. This figure agrees in order of magnitude with other estimates of the electric field in the magnetosphere.

*The existence and structure of electric fields in the magnetosphere are discussed, for example, in [133,148-151]. Direct measurements of the electric field in remote regions of the magnetosphere entail considerable difficulties which will take a considerable amount of time to overcome.

resonator. By R one can apparently mean the distance from the center of the earth to the subsolar point of the boundary of the magnetosphere. The great complexity of the resonant systems makes it difficult to analyze theoretically the connection between T and R. In this case, therefore, the empirical approach to the problem is fully justified.

The dependence of T on R, obtained by comparing Pc2–4 observations with satellite data concerning the position of the subsolar boundary of the magnetosphere, can be represented in the form[52]

$$T = T_0\left(\frac{R}{R_0}\right)^\nu, \qquad (38)$$

where $T_0 \approx 30$ sec, $R_0 \approx 10$ earth's radii, and $\nu \approx 4.5$ (Fig. 26). Since the Pc2–4 pulsations are observed on the illuminated side of the earth practically continuously, formula (38) makes it possible to determine the position of the boundary at practically any instant of time.

The importance of this diagnostics method cannot be overestimated. The point is that the position of the boundary can change in a predictable manner during the period between two successive loops of a satellite

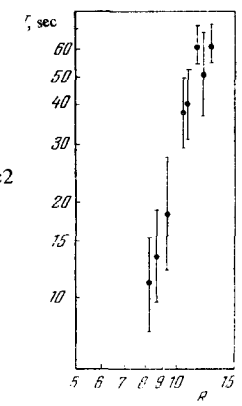

FIG. 26. Dependence of the period of Pc2 – 4 on the position of the boundary of the magnetosphere.

that crosses the surface of the geomagnetic cavity, i.e., the direct measurements have a low resolution in time. On the other hand, measurements based on pulsation data, although less accurate, make it possible to trace the position of the boundary continuously.

The possibility of monitoring the position of the boundary of the magnetosphere is of importance also for the investigation of the pulsations themselves. For example the Pc2—4 pulsations vanish sometimes after sudden negative si⁻ pulses. Understandably, formula (38) cannot be used in such cases to estimate R′ after si⁻. We take into account, however the fact that the magnitude of the sudden pulse on the equator is equal to[153]

$$\Delta H = \frac{\Delta H^*}{(R/10)^3}\left[\left(\frac{R}{R'}\right)^3 - 1\right], \qquad (39)$$

where R is the position of the boundary prior to si, and $\Delta H^* \approx 37\ \gamma$. Combining (38) with (39), we obtain[154]

$$R' \approx 10\left[\left(\frac{T_0}{T}\right)^{3/\nu} + \frac{\Delta H}{\Delta H^*}\right]^{-1/3}, \qquad (40)$$

where T is the period of the pulsations prior to si⁻. An analysis of the dependence of the probability of vanishing of the pulsations on R′ has made it possible to understand the nature of this effect[131].

3.2. Dimensions of the nighttime closed cavity. The magnetosphere is strongly asymmetrical with respect to the plane of the morning and evening meridians. The external force lines are blown by the solar wind into a long tail, and remain open up to distances at least several dozen earth's radii. The axis of the tail, naturally, does not take part in the daily rotation of earth. On the other hand, the internal closed force lines rotate together with the earth (see Fig. 21).

The asymmetry of the magnetosphere becomes manifest not only in the characteristic form of its outer surface, but also in the asymmetry of the form of the separation boundary between the closed and open lines. Thus, whereas in the noontime sector the separation boundary crosses the earth's surface at the latitude $\varphi_{day} \sim 78°$, in the midnight sector the latitude of the intersection lies closer to the equator, $\varphi_{night} \sim 67°$. In other words, the closed force lines extend to smaller distances on the night side than on the day side.

The question of the position and displacements of the boundary of the closed force lines is of fundamental significance in the theory of the radiation belts and in the general theory of magnetospheric dynamics. On the day side, the boundary of the closed lines practically coincide with the boundary of the magnetosphere R, for which land-based diagnostic methods were described in the preceding section. Although the position of the boundary of the closed lines of the night side φ_{night} is indeed connected in a definite manner with R, this connection is of the correlation type, so that to assess the changes of φ_{night} it is desirable to have an independent source of information.

An effective tool for investigating the nighttime magnetosphere is provided by the auroras; the instantaneous picture of the auroras is an oval whose outline of which is close to the line of intersection of the earth with the boundary surface that separates the closed magnetosphere lines from the force lines of the tail[39,146]. However, meaningful investigations of the auroras call for the organization of an extensive network of observatories equipped with relatively complicated apparatus, and the reduction of the primary observation material is a rather laborious process. At the same time, many general properties of the dynamic displacements of the nighttime boundary of the magnetosphere can be investigated by using geomagnetic-pulsation data.

The nighttime hemisphere is characterized by trains of Pi2 oscillations occurring most frequency in the near-midnight hours. It is probable that the period of the trains is determined by the dimensions of the closed cavity of the magnetosphere. A detailed investigation of this connection has only been started recently, in view of the great variety and complexity of the processes that occur in the night time magnetosphere. A statistical analysis shows that the period of Pi2 decreases with increasing magnetic disturbance[46-51]. For the development of diagnostic methods, however, further research is necessary with emphasis on individual comparisons of the positions of the oval zone of the auroras or of the outer boundary of the radiation belt with the spectrum of the oscillation trains.

4. Parameters of the Solar Wind

4.1. Wind velocity and structure of interplanetary fields. Almost the entire set of physical processes in a magnetosphere is governed by variations of the interplanetary conditions in the immediate vicinity of the earth. It can be stated that the earth and its magnetosphere are a giant space probe, sensitively responding to changes of the parameters of the outer medium. From the point of view of the specialist engaged in the diagnostics of cosmic plasma from data obtained by land-based observations, an investigation of the magnetosphere itself is equivalent to the study of the properties of this colossal instrument. Much is still to be done in this direction, but the progress already made allows us to formulate the main problems and to report some preliminary results.

First, the pulsation data concerning the position and displacement of the boundary of the magnetosphere contain indirect information about the dynamic pressure ($\sim NU^2$) of the solar wind. If it is recognized that the concentration of the interplanetary plasma N and the rate of its radial expansion U are somehow interconnected, then it becomes obvious that U can be estimated from data on the period of the Pc2-4 pulsations. Indeed, measurements have shown that the coefficient of the correlation between T and U is quite large ($r = 0.733 \pm 0.166$), and the relation between these quantities can be represented in the form[156]

$$U\,(\text{km/sec}) = (850 \pm 15) - (9.5 \pm 0.81)\,T\,(\text{sec}). \qquad (41)$$

The results of the comparison of the periods Pc2-4 with the velocity of the solar wind is given in Fig. 27. The dashed curve is a plot of (41). This figure is useful for estimating the wind velocity in time intervals when there are no direct measurements for some reason or another.

The fading of the Pc2-4 amplitude is due to changes of the orientation of the interplanetary magnetic field[54]

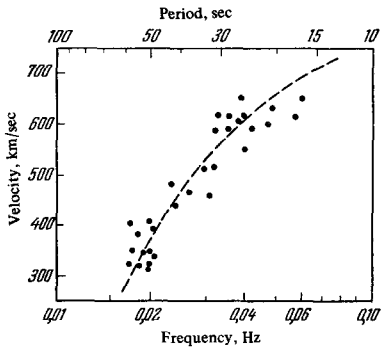

FIG. 27. Dependence of the period of Pc2 – 4 on the solar-wind velocity. The wind velocity is taken from the data of the rocket "Mariner-2." The pulsations are from the data of the Borok Observatory.

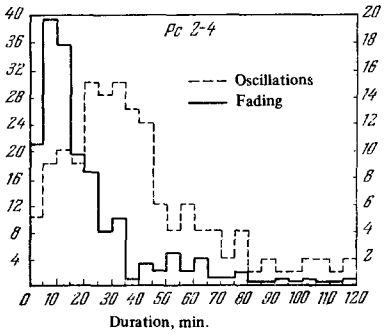

FIG. 28. Duration distribution of the fading (left scale) and oscillations of Pc2 – 4 (right scale). The plot contains information concerning the distribution of the inhomogeneities of the interplanetary field.

(see Fig. 11). This fact enables us to speak of the possibility of tentatively estimating the inhomogeneities of the interplanetary field from land-based pulsation observations.

The structure of the magnetic field in interplanetary space is quite complicated. It includes a set of inhomogeneities of various scales and various characters. The smooth projection of the force lines on the ecliptic plane has the form of spirals, the angle of inclination of which to the radius vector from the sun on the earth's orbit is $\psi \sim 50°$[53]. Since the fading of the Pc2–4 amplitude occurs when the radial component of the interplanetary field vanishes, data on the fading make it possible to evaluate the distribution of the angles of rotation of the force lines at $\Delta\psi \sim 40°$. Figure 28 shows the duration distribution of the fading and oscillations of Pc2–4. On the average, the fading duration is $t_1 \sim 6 \times 10^2$ sec, and that of the oscillations is $t_2 \sim 1.8 \times 10^3$ sec. If it is assumed that the inhomogeneities are transported past the earth with the velocity of the solar wind, then the corresponding scales are equal to $l_1 \sim 3 \times 10^{10}$ cm and $l_2 \sim 9 \times 10^{10}$ cm. The ratio l_2/l_1 is of the order of 3.

One can advance the hypothesis that the inhomogeneities recorded in this manner are precisely those which determine the character of the angular distribution of the solar cosmic rays during the first anisotropic stage of their appearance[157]. This hypothesis is checked in the following manner. On the one hand, the inhomogeneities are analyzed from the data on the direction of arrival of cosmic rays of various energies following a concrete flare on the sun. On the other hand, the dimensions of the inhomogeneities are estimated from the modulation of Pc2–4 during the time interval preceding the flare. For example, during the flare of 28 September 1961, the ratios l_2/l_1 were ~2.5 (cosmic rays) and ~2.25 (pulsations), i.e., a distinct correspondence does exist.

4.2. Concerning new indices of geomagnetic activity. The search for quantitative measures—activity indices—characterizing the disturbance of the magnetosphere has been going on for a long time (several decades). The indices u, A, Q, C, Kp, and others, based on standard records of magnetic observatories, are well known[158]. These indices characterize the variation of the components of the geomagnetic field within a chosen averaging interval (one hour, three hours, one day, one month, one year, etc.).

The need for convenient measures of the geomagnetic activity arises in the solution of a large number of problems. On the basis of the correlation between the solar and geomagnetic activity, methods are being developed for forecasting magnetic and ionospheric disturbances that interfere with radio communication and magnetic navigation. An analysis of 27-day, seasonal, 11-year, and secular variations of the activity contributes to a better understanding of the physical nature of the sun-earth communication, etc.

The progress in hydromagnetic diagnostics of the magnetosphere gives grounds for introducing a series of new activity indices[10]. We mention here the indices $\mathfrak{R}$, $\mathfrak{N}$, $\mathfrak{P}$, and $\mathfrak{S}$, which are constructed in accordance with data on the pulsations Pc2–4, Pi2, Pc1, and Pi1 respectively. In conjunction with the classical indices, they make it possible to describe quite completely the state of the magnetosphere and of the interplanetary medium.

The index $\mathfrak{R}$ is made up by averaging the periods of the daytime pulsations Pc2–Pc4 over three hours, and has a distinct physical meaning. It is equal to the deviation of the position of the subsolar boundary of the magnetosphere from the mean value: $\mathfrak{R} = R_{av} - R$. Under certain assumptions, the $\mathfrak{R}$ index can be related to the velocity of the solar wind (Table III).

The $\mathfrak{S}$ index is equal to the number of trains of Pi2 oscillations in a three-hour interval. It characterizes the activity of the nighttime magnetosphere, which in turn depends on the general hydromagnetic setup in the cosmic vicinity of the earth.

The $\mathfrak{P}$ index is equal to the logarithm of the duration of the Pc1 series, multiplied by the mean-squared oscillation amplitude. This quantity is proportional to the logarithm of the energy of the hydromagnetic waves in the Pc1 band.

The $\mathfrak{E}$ index, which is equal to const $\cdot \omega^{-1/3}(d\omega/dt)$, is made up from data on the growing-amplitude pulsations and is an individual characteristic of each magnetic storm.

Table III

$\mathfrak{R}$	–2	–1	0	+1	+2
U, km/sec	250	300	450	600	800

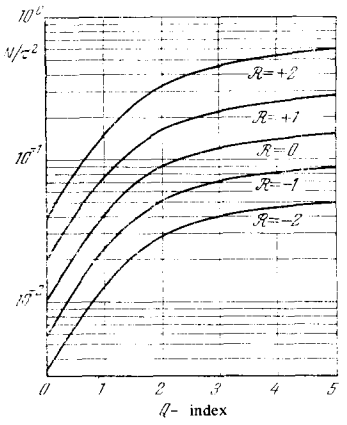

FIG. 29. Diagnostic diagram. The concentration of the plasma in the tail of the magnetosphere can be estimated from data on the repetition period of the pulses τ (in minutes) if the Q and $\mathcal{R}$ indices are known.

To construct the indices, use is made of continuous recordings obtained at the observatories in Borok (Yaroslavl' oblast'), Petropavlovsk (Kamchatka), and Soroa (Cuba). As the earth rotates, the observatories enter in sequence in their "working interval" of local time. This makes it possible to eliminate the dependence of the periods and of the amplitudes of the oscillations on the local time.

Figure 29 shows a concrete example of the use of indices for the diagnostics of the plasma concentration in the tail (see Ch. III, Sec. 1.2). The abscissas represent the Q-index, which depends on the position of the oval zone of the auroras[146]. The plot makes it possible to estimate N from data on the repetition periods of the Pi1 flashes when the Q and $\mathcal{R}$ indices are known[137].

IV. CONCLUSION

Historically it has turned out so that geomagnetic pulsations were the first electromagnetic waves recorded by man. It is surprising that their high information content was recognized only very recently. This is to be regretted, but is it meaningful to use pulsations for the diagnostics of the magnetosphere in our days, when dozens of satellites bearing scientific instruments travel around the earth?

This question should definitely be answered in the affirmative. Hardly anyone proposes seriously that the significance of land-based observation service can be decreased to some degree by installing magnetometers on satellites for the purpose of investigating the regular magnetic field, or by placing astronomic instruments outside the dense atmosphere. Satellite and land-based research methods are not competitive, but rather complement each other. In this light, it is quite obvious that pulsations and other low-frequency radiations are an important auxiliary research tool. The possibility of continuous and prolonged observations of the state of the magnetosphere with the aid of relatively simple apparatus is an undisputable practical advantage of low-frequency diagnostic methods.

As in any field that survives the establishment period, unexpected prospects can arise at any instant of time, whereas other possibilities, which seem highly promising at the present time, may subsequently turn out to be illusory. In one way or another, although individual properties of geomagnetic pulsations still remain puzzling, and the theory of land-based diagnostics of the magnetosphere is making only its first steps, the progress already made makes it possible to state with assurance that observation of pulsations will uncover new ways of further investigations of the magnetosphere.

The developments of this field will depend on the progress made in solving a large number of fundamental theoretical and experimental problems. In particular, further calculations of the spectrum of the natural oscillations of realistic models of the magnetosphere, of the critical frequency, of the phase velocity and damping of hydromagnetic waves in the ionospheric waveguide, of the coefficient of penetration of the waves to the earth's surface through the ionosphere, etc., are highly desirable, The experimental facts and theoretical estimates indicate that the mechanisms of pulsation excitation cannot be fully understood within the framework of the linear theory. In other words, it becomes necessary to solve complicated nonlinear problems in the interpretation of the pulsations.

Many important properties of the pulsations can be clarified by comprehensive and correlated research in a global network of land-based observatories, and by observations of the hydromagnetic waves directly in outer space. The development of diagnostic methods will apparently be connected with extensive utilization of computer technology both for the interpretation of the pulsations and for the solution of the corresponding inverse problems. This in turn requires the use of pulsation registration methods that permit the insertion of the records directly into the computers.

The investigation of geomagnetic pulsations is continuing, and there are grounds for assuming that their observation will become not only convenient but also a quantitative method of measuring the parameters of the outer space next to the earth.

[1] V. A. Troitskaya, J. Geophys. Res. 66, 5 (1961).
[2] N. Brice, Nature (London) 206, 283 (1965).
[3] B. N. Gershman and V. A. Ugarov, Usp. Fiz. Nauk 72, 235 (1960) [Sov. Phys.-Usp. 3, 743 (1961)].
[4] B. N. Gershman and V. Yu. Trakhtengerts, Usp. Fiz. Nauk 89, 201 (1966) [Sov. Phys.-Usp. 9, 414 (1966)].
[5] Y. Kato and T. Watanabe, Sci. Repts. Tohoku Univ., Ser. 5, 8, 157 (1957).
[6] J. A. Jacobs and K. Sinno, Geophys. J. 3, 333 (1960).
[7] J. A. Jacobs and K. O. Westphal, in: Physics and Chemistry of the Earth, (L. H. Ahrens et al., Eds.), Vol. 5, p. 253, Pergamon Press, 1963.
[8] V. A. Troitskaya, Research in Geophysics, (H. Odishaw, Ed.), Vol. 1, p. 485, M. I. T. Press, 1964.
[9] V. A. Troitskaya, Solar-Terrestrial Physics, (J. W. King and W. S. Newman, Eds.), ch. VII, Acad. Press, London—New York, 1967.
[10] V. A. Troitskaya and A. V. Gul'elmi, Space Sci. Rev. 7, 689 (1967).
[11] R. Gendrin, Space Sci. Rev. 7, 314 (1967).
[12] W. H. Campbell, Physics of Geomagnetic Phenomena (S. Matsushita and W. H. Campbell, Eds.), Vol. 2, p. 821, Acad. Press, 1967.
[13] V. A. Troitskaya and O. V. Bolshakova, Report

presented at Symposium on U. L. F. Electromagnetic Fields, Boulder, Colorado, 1964.
[14]V. A. Troitskaya, O. V. Bol'shakova, A. V. Gul'el'mi, and É. T. Matveeva, Geomagnitnye issledovaniya (Geomagnetic Research) 9, 15 (1967).
[15]V. A. Troitskaya, O. V. Bol'shakova, and É. T. Matveeva, Geomagnetizm i aéronomiya 6, 533 (1966).
[16]V. A. Troitskaya and A. V. Gul'el'mi, Vest. AN SSSR No. 6, 127 (1968).
[17]V. A. Troitskaya,and A. V. Gul'el'mi, Report Presented in Inter-Union Symposium on Cosmical Physics, Washington, 1968.
[18]R. Gendrin and V. A. Troitskaya, Radio Sci. 69D, 1107 (1965); CNFRA, No. 21 (1967).
[19]E. M. Wescott and V. P. Hessler, Nature 212, 170 (1966).
[20]O. V. Bolshakova, V. A. Troitskaya, and V. P. Hassler, Ann. Geophys. 23, N 3 (1968).
[21]V. A. Troitskaya, Dokl. Akad. Nauk SSSR 99, 231 (1953).
[22]J. A. Jacobs, Y. Kato, S. Matsushita, and V. A. Troitskaya, J. Geophys. Res. 69, 180 (1964).
[23]V. A. Troitskaya, Geomagnetizm i aéronomiya 4, 615 (1964).
[24]L. R. Tepley and R. C. Wentworth, J. Geophys. Res. 67, 3317 (1962).
[25]L. Tepley, Radio Sci. 69D, 1089 (1965).
[26]K. Yanagihara, J. Geophys. Res. 68, 3383 (1963).
[27]R. Gendrin, S. Lacourly, M. Gokhberg, O. Malevskaya, and V. A. Troitskaya, Ann. Geophys. 22, 329 (1966).
[28]V. B. Lyatskiĭ and V. P. Selivanov, Geomagnetizm i aéronomiya 6, 162 (1966).
[29]V. A. Troitskaya, L. N. Baranskiĭ, P. A. Vinogradov, A. V. Sobolev, and S. I. Solov'ev, Geomagnetizm i aéronomiya 8, 726 (1968).
[30]É. T. Matveeva and V. A. Troitskaya, Geomagnetizm i aéronomiya 5, 1079 (1965).
[31]R. C. Wentworth, L. Tepley, K. D. Amundsen, and R. R. Heacock, J. Geophys. Res. 71, 1492 (1966).
[32]L. N. Baranskiĭ, B. N. Kazak, and L. A. Geller, Dokl. Akad. Nauk SSSR 177, 85 (1967).
[33]J. F. Kenney and H. B. Knaflich, J. Geophys. Res. 72, 2857 (1967).
[34]R. R. Heacock and V. P. Hessler, J. Geophys. Res. 70, 1103 (1965).
[35]S. Kokubun and T. Oguti, J. Geomagn. Geoelectr. 20 (1968).
[36]R. Mc Pherrons and S. Ward, J. Geophys. Res. 72, 393 (1967).
[37]R. C. Wentworth, J. Geophys. Res. 69, 2291 (1964).
[38]T. A. Plyasova-Bakunina and É. T. Matveeva, Geomagnetizm i aéronomiya 8, 189 (1968).
[39]S. Akasofu, Scientific American 213 (6), 55 (1965).
[40]O. M. Raspopov, V. A. Troitskaya, R. Zhandren, B. N. Kazak, and Zh. Loran, Geomagnetizm i aéronomiya 7, 864 (1967).
[41]R. Gendrin, S. Lacourly, V. A. Troitskaya, M. Gokhberg, and R. V. Shepetnov, Planet. Space Sci. 15, 1239 (1967).
[42]H. B. Knaflich and J. F. Kenney, Boeing Sci. Res. Lab., D1-82-0616 (1967).
[43]R. R. Heacock, J. Geophys. Res. 72, 399 (1967).
[44]L. Tepley,and K. D. Amundsen, J. Geophys. Res. 70, 234 (1965).
[45]O. V. Bol'shakova and K. Yu. Zybin, Geomagnitnye issledovaniya 6, 79, 87 (1964).
[46]O. V. Bol'shakova, Dissertation, Moscow, 1965.
[47]K. Yu. Zybin, Geomagnitnye issledovaniya 9, 63 (1967).
[48]G. Rostoker, J. Geophys. Res. 72, 2032 (1967).
[49]O. M. Raspopov, Geomagnetizm i aéronomiya 9, (1969).
[50]O. M. Raspopov, V. A. Troitskaya, R. Shlish, I. S. Lizunkova, B. N. Kazak, and V. K. Koshelevskiĭ, Geomagnetizm i aéronomiya 7, 858 (1967).
[51]R. V. Shchepetnov, Dissertation, Moscow, 1968.
[52]O. V. Bol'shakova, Geomagnetizm i aéronomiya 5, 775, 868 (1965).
[53]L. J. Cahill, Jr., Scientific American, 212 (3), 58 (1965).
[54]O. V. Bol'shakova and V. A. Troitskaya, Dokl. Akad. Nauk SSSR 180, 343 (1968).
[55]J. M. Wilcox, Space Sci. Rev. 8, 258 (1958).
[56]A. I. Ol', Trudy AANII 241, 39 (1962);Geomagnetizm i aéronomiya 3, 113 (1963).
[57]T. Saito and S. Matsushita, Planet, Space Sci. 15, 573 (1967).
[58]D. Brooks, J. Atmosph. Terr. Phys. 29, 589 (1967).
[59]L. D. Landau and E. M. Lifshitz, Élektrodinamika sploshnykh sred, Fizmatgiz, 1959 (Electrodynamics of Continuous Media, Addison-Wesley, 1960).
[60]V. L. Ginzburg, Rasprostranenie élektromagnitnykh voln v plazme (Propagation of Electromagnetic Waves in a Plasma), Fizmatgiz, 1960.
[61]V. P. Silin and A. A. Rukhadze, Élektromagnitnye svoĭstva plazmy i plazmopodobnykh sred (Electromagnetic Properties of Plasma and Plasmalike Media), Gosatomizdat, 1961.
[62]V. D. Shafranov, Voprosy teorii plazmy (Problems of Plasma Theory) 3, 3 (1963).
[63]A. I. Akhiezer, I. A. Akhiezer, R. V. Polovin, A. G. Sitenko, and K. N. Stepanov, Kollektivnye kolebaniya v plazme (Collective Oscillations in Plasma), Atomizdat, 1964.
[64]T. Stix, Theory of Plasma Waves, McGraw-Hill, 1962
[65]B. A. Tverskoĭ, Dinamika radiatsionnykh poyasov (Dynamics of the Radiation Belts), Nauka, 1968.
[66]H. A. Taylor, H. C. Brinton, and C. R. Smith, J. Geophys. Res. 70, 5769 (1965).
[67]M. A. Gintsburg, Geomagnetizm i aéronomiya 2, 642 (1962).
[68]D. A. Gurnett, S. D. Shawhan, N. M. Brice, and R. L. Smith, J. Geophys. Res. 70, 1665 (1965).
[69]A. V. Gul'el'mi, Dokl. Akad. Nauk SSSR 174, 1076 (1967).
[70]R. L. Dowden, Planet. Space Sci. 13, 761 (1965).
[71]J. A. Jacobs and T. Watanabe, J. Atmosph. Terr. Phys. 26, 825 (1964).
[72]T. Obayashi, J. Geophys. Res. 70, 1069 (1965).
[73]R. C. Wentworth, J. Geomagn. Geoelectr. 18, 257 (1966).
[74]R. L. Dowden and M. W. Emery, Planet. Space Sci. 13, 773 (1965).
[75]T. Watanabe, J. Geophys. Res. 70, 5839 (1965).
[76]H. B. Liemohn, J. F. Kenney, and H. B. Knaflich.

Boeing Sci. Res. Lab. D1-82-0615 (1967).
[77]A. V. Gul'el'mi, Geomagnetizm i aéronomiya 9, 179 (1969).
[78]V. A. Troitskaya, É. T. Matveeva, K. G. Ivanov, and A. V. Gul'el'mi, Geomagnetizm i aéronomiya 8, 980 (1968).
[79]A. V. Gul'el'mi, Presented at Inter-Union Symposium on Solar-Terrestrial Physics, Belgrade, 1966.
[80]R. L. Dowden, Planet. Space Sci. 14, 1273 (1966).
[81]M. S. V. Gopal Rao and H. G. Booker, J. Geophys. Res. 68, 387 (1963).
[82]D. L. Carpenter, J. Geophys. Res. 71, 693 (1966).
[83]K. I. Gringauz, Geofiz. byulleten' 14, 110 (1965).
[84]A. V. Gul'el'mi, Geomagnetizm i aéronomiya 3, 754 (1963).
[85]A. V. Gul'el'mi, Geomagnetizm i aéronomiya 7, 344 (1967).
[86]A. V. Gul'el'mi, Ann. Geophys. 24, (3) 761 (1968).
[87]J. W. Dungey, in: Geophysics, the Earth's Environment (Les Houches), p. 505, Gordon and Breach, 1963.
[88]Yu. L. Moskvin and D. A. Frank-Kamenetskiĭ, Dokl. Akad. Nauk SSSR 174, 1079 (1967). Geomagnetizm i aéronomiya 7, 144 (1967).
[89]A. N. Tikhonov and D. N. Shakhsuvarov, Uzv. AN SSSR, ser. geofiz. 4, (1956).
[90]B. M. Yanovskiĭ, Zemnoĭ magnetizm (Terrestrial Magnetism), LGU, 1964.
[91]M. N. Berdichevskiĭ, Élektricheskaya razvedka (Electric Prospecting), Nedra, 1968.
[92]R. L. Carovillano, H. R. Radosky, and J. F. McClay, Phys. Fluids 9, 1860 (1966).
[93]L. L. Van'yan and K. Yu. Zybin, Kosmich. issledovaniya 4, 935 (1966).
[94]G. MacDonald, J. Geophys. Res. 66, 3639 (1961).
[95]K. O. Westphal,and J. A. Jacobs, Geophys. J. 6, 360 (1962).
[96]H. G. Radoski,and R. L. Carovillano, Phys. Fluids 9, 285 (1966); 10, 225 (1967).
[97]H. R. Radoski, J. Geomagn. Geoelectr. 19, 1 (1967).
[98]W. E. Francis and R. Karplus, J. Geophys. Res. 65, 3593 (1960).
[99]R. Karplus, W. E. Francis, and A. J. Dragt, Planet. Space Sci. 9, 771 (1962).
[100]S.-I. Akasofu, Radio Sci. 69D, 361 (1965).
[101]C. Greifinger and Ph. Greifinger, J. Geophys. Res. 70, 2217 (1965).
[102]E. C. Field and C. Greifinger, J. Geophys. Res. 70, 4885 (1965); 71, 3223 (1966).
[103]J. Bochníček, Studia Geophys. Geod. 11, 65 (1967).
[104]R. N. Manchester, J. Geophys. Res. 71, 3749 (1966).
[105]L. Tepley and R. K. Landshoff, J. Geophys. Res. 71, 1499 (1966).
[106]D. N. Chetaev and M. G. Savin, Geomagnitnye issledovaniya 10, (1969).
[107]D. N. Chetaev, Dokl. Akad. Nauk SSSR 174, 775 (1967) [Sov. Phys.-Dokl. 12, 555 (1967)].
[108]V. M. Davydov, Geomagnetizm i aéronomiya 9, (1969).
[109]W. H. Campbell and S. Matsushita, J. Geophys. Res. 67, 555 (1962).
[110]G. A. Loginov, M. I. Pudovkin, and R. G. Skrynnikov, Geomagnetizm i aéronomiya 3, 59 (1963).
[111]J. M. Cornwall, J. Geophys. Res. 70, 61 (1965); 71 2185 (1966).
[112]C. F. Kennel and H. E. Petschek, J. Geophys. Res. 71, 1 (1966).
[113]H. B. Liemohn, J. Geophys. Res. 72, 39 (1967).
[114]A. V. Gul'el'mi, Geomagnetizm i aéronomiya 8, 412 (1968).
[115]F. Z. Feĭgin and V. L. Yakimenko, Geomagnetizm i aéronomiya 9, (1969).
[116]M. A. Gintzburg, Izv. AN SSSR, ser. geofiz. 11, 1679 (1961).
[117]A. Nishida, J. Geophys. Res. 69, 947 (1964).
[118]R. Gendrin, J. Geophys. Res. 70, 5369 (1965).
[119]A. V. Gul'el'mi, Geomagnetizm i aéronomiya 6, 1129 (1966).
[120]J. A. Jacobs and T. Watanabe, J. Atmosph. Terr. Phys. 28, 235 (1966); Planet. Space, Sci 15, 799 (1967).
[121]A. Hruška, J. Geophys. Res. 71, 1377 (1966); Studia Geoph. Geod. 11, 235 (1967).
[122]B. E. Bryunelli and V. B. Lyatskiĭ, Geomagnetizm i aéronomiya 7, 682 (1967).
[123]G. Atkinson and T. Watanabe, Earth and Planet. Sci. Lett. 1, 89 (1966).
[124]S. N. Vernov, Issledovaniya kosmicheskogo prostranstva (Investigations of Outer Space), Nauka, 1965, p. 277.
[125]V. A. Troitskaya, É. T. Matveeva, and A. V. Gul'el'mi, Geomagnetizm i aéronomiya 9, (1969).
[126]V. A. Troitskaya and N. F. Mal'tseva, Geomagnetizm i aéronomiya 7, 1124 (1967).
[127]S. Chapman, in: Geophysics, the Earth's Environment (les Houches), Gordon and Breach, 1963.
[128]M. Kozlowski, J. Geophys. Res. 68, 4421 (1963).
[129]S. I. Syrovatskiĭ (cited in[59], p. 287).
[130]D. Fairfield, J. Geophys. Res. 72, 5865 (1967).
[131]V. A. Troitskaya, R. V. Shchepetnov, and A. V. Gul'el'mi, Geomagnetizm i aéronomiya 9, (1969).
[132]T. Obayashi, in: Solar-Terrestrial Physics (J. W. King and W. S. Newman, Eds.), Acad. Press, London-New York, 1967.
[133]V. P. Shabansky, Space Sci. Rev. 8, 366 (1968).
[134]J. H. Piddington, J. Atmosph. Terr. Phys. 29, 87 (1967).
[135]K. G. Ivanov and N. V. Mikerina, Geomagnetizm i aéronomiya 7, 1036 (1967).
[136]R. Z. Sagdeev, Voprosy teorii plazmy 4, 20 (1964).
[137]V. A. Troitskaya, A. V. Gul'el'mi, and R. V. Shchepetnov, Trudy Mezhdunarodnogo soveshchaniya po geomagnitnym vozmushcheniyam (Proc. Internat. Conf. on Geomagnetic Disturbances), KrAO, 1969.
[138]Ya. L. Al'pert, Usp. Fiz. Nauk 90, 405 (1966) [Sov. Phys.-Usp. 9, 787 (1967).
[139]L. R. O. Storey, Phyl. Trans. Roy. Soc. London A246, 113 (1953).
[140]T. Obayashi, Ann. Geophys. 14, 464 (1958).
[141]A. V. Gul'el'mi, Geomagnetizm i aéronomiya 6, 132 (1966); 7, 442 (1967).
[142]T. Kitamura, Rept. Ionosph. Space Res. Japan 19, 21 (1965).
[143]J. A. Jacobs and T. Kitamura, Trans. Amer. Geophys. Union 47, 73 (1966).
[144]V. I. Slysh, Kosmich, issledovaniya 3, 760 (1965).
[145]T. Obayashi, Rep. Ionosph. Space Res. Japan 19, 2

(1965).
[146] Ya. I. Fel'dshteĭn and G. V. Starkov, Planet. Space Sci. 15, 209 (1967); Geomagnetizm i aéronomiya 7, 62 72 (1967).
[147] A. V. Gul'el'mi, Trudy Vsesoyuznogo soveshchaniya po rezul'tatam MGSS (Proc. of All-union Conference on the Results of IYQS), Moscow, 1969.
[148] L. A. Frank, J. Geophys. Res. 72, 1905 (1967).
[149] N. M. Brice, J. Geophys. Res. 72, 5193 (1967).
[150] O. E. Dubatenko, M. I. Pudovkin, and O. I. Shumilov, Geomagnetizm i aéronomiya 8, 303 (1968).
[151] D. L. Carpenter and K. Stone, Planet. Space Sci. 15, 395 (1967).
[152] V. A. Troitskaya, R. V. Shchepetnov, and A. V. Gul'el'mi, Geomagnetizm i aéronomiya 8, 798 (1968).
[153] G. D. Mead, J. Geophys. Res. 49, 1181 (1964).
[154] V. A. Troitskaya, R. V. Shchepetnov, and A. V. Gul'el'mi, Dokl. Akad. Nauk SSSR 182, 79 (1968) [Sov. Phys.-Dokl. 13, (1969)].
[155] L. Bierman, Sitzber. Bayerische Akad. Wiss. 37, (1965).
[156] O. V. Bol'shakova, Astron. Zh. 42, 859 (1965) [Sov. Phys.-AJ 9, 666 (1966)].
[157] L. I. Dorman, Variatsiya kosmicheskikh lucheĭ i issledovanie kosmosa (Cosmic Ray Variation and Outer Space Research), AN SSSR, 1963.
[158] S. Chapman and J. Bartels, Geomagnetism, Oxford Univ. Press, 1951.

Translated by J. G. Adashko